

## Repeated Divergence in Opsin Genes Expression Mirrors Photic Habitat Changes in Rapidly Evolving Crater Lake Cichlid Fishes

César Bertinetti<sup>1,2</sup>, Andreas Härer<sup>1,3</sup>, Nidal Karagic<sup>1,4</sup>, Axel Meyer<sup>1</sup>, Julián Torres-Dowdall<sup>1,2</sup>.

<sup>1</sup> Zoology and Evolutionary Biology, Department of Biology, University of Konstanz, Konstanz, Germany

<sup>2</sup> Department of Biological Sciences, University of Notre Dame, Notre Dame, IN, USA

<sup>3</sup> current address: School of Biological Sciences, Department of Ecology, Behavior, & Evolution, University of California San Diego, La Jolla, CA, USA

<sup>4</sup> current address: Biotechnological Institute, University of Helsinki, Helsinki, Finland

Corresponding author: Julián Torres-Dowdall, Email: [torresdowdall@nd.edu](mailto:torresdowdall@nd.edu)

ORCID Cesar Bertinetti: 0000-0001-5454-5688

ORCID Andreas Härer: 0000-0003-2894-5041

ORCID Nidal Karagic: 0000-0003-3575-3558

ORCID Axel Meyer: 0000-0002-0888-8193

ORCID Julián Torres-Dowdall: 0000-0003-2729-6246

Article type: Major article, 7427 words

The article includes 4 Figures, 10 Supplementary Figures, 6 Supplementary Tables and [Dryad Repository](#) (Code + Data)

Running head: Repeated Divergence in Opsin Expression

## Abstract

Selection pressures differ along environmental gradients and traits tightly linked to fitness (e.g., the visual system) are expected to track such variation. Along gradients, adaptation to local conditions might be due to heritable and non-heritable, environmentally induced variation. Disentangling these sources of phenotypic variation requires studying closely related populations in nature and the laboratory. The Nicaraguan lakes represent an environmental gradient in photic conditions from clear crater lakes to very turbid great lakes. From two old, turbid great lakes, Midas cichlid fish (*Amphilophus cf. citrinellus*) independently colonized seven isolated crater lakes of varying light conditions, resulting in a small adaptive radiation. We estimated visual sensitivities variation along this photic gradient by measuring cone opsin gene expression among lake populations. Visual sensitivities observed in all seven derived crater lake populations shifted predictably in direction and magnitude, repeatedly mirroring changes in photic conditions. Comparing wild-caught and laboratory-reared fish revealed that 48% of this phenotypic variation is genetically determined and evolved rapidly. Decreasing intrapopulation variation as environments become spectrally narrower suggests that different selective landscapes operate along the gradient. We conclude that the power to predict phenotypic evolution along gradients depends on both the magnitude of environmental change and the selective landscape shape.

**Keywords:** local adaptation, phenotypic evolution, environmental gradient, sensory ecology, visual sensitivity

## Introduction

Abiotic factors are widely recognized selective agents influencing biological diversity by affecting fitness and thus driving evolution by natural selection (Endler 1986; Haldane 1948; Maccoll 2011; Schluter 2000). Evolutionary theory predicts that, provided that enough genetic variation for a trait exists, phenotypes under selection would be expected to match local optima, particularly in the

absence of gene flow (Fisher 1930; Kawecki and Ebert 2004; Williams 1966). Most commonly, local adaptation has been studied focusing on the ends of the environmental continuum in a dichotomous way (e.g., Barrett et al. 2008; Filchak et al. 2000; Girvan and Braithwaite 1998; Hoekstra et al. 2004; Reznick and Endler 1982; Tobler et al. 2018). Although analyzing extreme habitats increases the power to detect adaptation, it might not suffice to explain the range of phenotypic variation observed across natural populations (Becker et al. 2006; Hereford and Winn 2008; Riesch et al. 2018). For instance, habitat conditions that vary in a continuous manner might result in gradual variation for selected traits (Endler 1977; Huxley 1938; Sotka 2008). Several classic studies have identified local adaptation along environmental gradients in different taxonomic groups (Bishop 1972; Clausen et al. 1948; Huey et al. 2000; McNeilly 1968; Mullen and Hoekstra 2008; Sand et al. 1995). Leveraging such systems allows us to test how closely organisms track environmental changes and contributes to broadening our understanding about the predictability of evolutionary outcomes (Blount et al. 2018; Losos 2018; Nosil et al. 2018). In theory, adaptive phenotypic evolution should mirror environmental pressures and facilitate contemporary evolution, especially in the presence of geographic barriers where gene flow cannot counteract the effect of selection (García-Ramos and Kirkpatrick 1997).

The visual system is a particularly fitting trait to study evolution by natural selection given its crucial role in fitness-related tasks such as mate choice, foraging behavior, predator avoidance, or conspecific recognition (Cronin et al. 2014). In particular, aquatic organisms are often exposed to an especially wide range of photic conditions (Kirk 2010). When traveling through water, light is strongly attenuated over short depths and depleted of certain wavelengths. This creates a diversity of photic environments found across aquatic ecosystems (Loew and McFarland 1990; Partridge and Cummings 1999). Therefore, aquatic organisms are a good candidate to study how visual systems respond to spectral variability, a key abiotic factor that can be quantified and compared across environments (Carleton et al. 2020). By addressing opposite ends of the photic

continuum, several studies in fish have reported divergence in the visual system between different light conditions (Fuller et al. 2004; Hahn et al. 2017; Marques et al. 2017; Rennison et al. 2016; Spady et al. 2005; Torres-Dowdall et al. 2017). In those studied cases, vision is tuned in a discrete manner by structural changes in key proteins or by regulating gene expression in response to different photic conditions. In contrast, studying a broader range of photic conditions allows testing how predictably phenotypes change in response to gradual environmental variation.

Color vision is initiated in response to light in cone photoreceptor cells found in the retina. Cone photoreceptors contain visual pigments, light-sensitive molecules consisting of an opsin protein bound to a chromophore (Bowmaker 1990). The amino acid residues of the opsin protein and the type of chromophore determine the probability of a visual pigment absorbing a photon of a given wavelength, in other words, the spectral sensitivity of the photoreceptor (Davies et al. 2012; Wald 1939). Therefore, the ability of organisms to detect color relies in the first place on the expression of cone opsin genes with different spectral sensitivities across photoreceptor cells (Carleton et al. 2020; Cronin et al. 2014; Johnsen 2012; Lythgoe 1979; Musilova et al. 2021; Schweikert et al. 2018). The wavelength-dependent photoreceptor signals are then processed downstream by bipolar and ganglion cells and finally in the brain to generate color perceptions (Baden 2021; Baden and Osorio 2019). Despite the complexity of the neural processes associated with color vision, the association between retinal expression of certain cone opsin genes and the overall visual sensitivity of an organism have been extensively studied (Baden 2021; Carleton and Yourick 2020; Cronin et al. 2014). For instance, sensitivity to ultraviolet light (UV) was described in several species based on behavioral experiments before the expression of UV-sensitive opsin genes (*sws1*) could be reliably quantified and the physiological relevance of *sws1* has been experimentally linked to foraging performance (Cronin and Bok 2016; Novales Flamarique 2016). Similar associations have been made for sensitivity to long-wavelength regions of the spectrum and the expression of red-sensitive cone opsin genes (Sakai et al. 2018; Smith

et al. 2012). The relationship between spectral sensitivity and the relative expression of cone opsin genes in the retina has also been demonstrated via electrophysiological measurements (Sabbah et al. 2010). Further, measurements of retinal opsin gene expression using quantitative real-time PCR (qPCR) have been shown to reflect the number of photoreceptors in each spectral class using RNA-fluorescence in-situ hybridization and to be correlated with RNA sequencing data (Härer et al. 2018; Karagic et al. 2018). Hence, while the detailed mechanisms involved in visual sensitivity still are a matter of ongoing research, there is a logical link between retinal opsin gene expression, the spectral sensitivity of the cone photoreceptors, and the overall visual sensitivity of the retina.

Due to both gene gains and losses and sequence divergence, the so-called visual opsins within the opsin gene family vary substantially across lineages, resulting in spectral sensitivities that extend over much of the visible spectrum (Yokoyama 2000). Among vertebrates, teleost fishes have a highly diverse number of visual opsins, with a median of six cone opsin genes found in their genomes (Musilova et al. 2019; Yokoyama 2008). Cichlid fishes (Family Cichlidae) typically possess seven cone opsin genes, three short-wavelength sensitive ones expressed in single cones (*sws1*, *sws2a*, *sws2b*) and four mid- to long-wavelength sensitive ones expressed in double cones (*rh2b*, *rh2a $\alpha$* , *rh2a $\beta$* , *lws*), although not all these genes are usually expressed simultaneously. In lineages of African cichlids, opsin genes seem to be expressed in fixed combinations, i.e., visual palettes (Carleton et al. 2010) with visual sensitivities being discretely distributed in either short- (*sws1*, *rh2b*, *rh2a*), middle- (*sws2b*, *sws2a*, *rh2a*), or long-wavelength (*sws2a*, *rh2a*, *lws*) clusters (Hofmann et al. 2009). The modularity of the palettes contrasts with visual sensitivities in some Neotropical cichlids, where opsin expression is not compartmentalized into palettes, but seems to be more tunable (Torres-Dowdall et al. 2021). Given that visual sensitivities represent an integrated phenotype comprised of a limited number of opsins, the distinct modularities described so far should mirror environmental gradients in different ways. If

visual sensitivities are constrained, modularity should result in a limited number of phenotypes along gradients (Hofmann et al. 2009; O'Quin et al. 2010). Instead, gradual phenotypic variation might be expected if visual sensitivities are not restricted to the modular expression of opsin genes (e.g., Torres-Dowdall et al. 2021). The degree to which visual sensitivities can be tuned will inevitably shape the variation available for natural selection to act upon and thus the phenotypic range in the wild.

A useful framework to study visual sensitivities in the wild is referred to as the “sensitivity hypothesis”, which states that organisms’ retinal sensitivities should be optimized to maximize sensitivity to the predominant background spectral regions (Bayliss et al. 1936; Clarke 1936; Crescitelli et al. 1985). Under this hypothesis, natural selection might favor visual sensitivities that match the local photic environment consequently shaping phenotypic variation (Bowmaker 1990; Cronin et al. 2014; Lythgoe 1979). Further, while spectrally narrow environments have only a small subset of wavelengths available for visual systems to exploit, broadband environments offer more spectral regions for visual sensitivities to diversify (Carleton et al. 2016; Loew 1995; O'Quin et al. 2010). As an analogy, one could regard photons as a resource available for pigments to be exploited (Stomp et al. 2007), where broadband photic environments represent multiple photon-rich spectral regions that contrast with the resource-poor tightly allocated photons in narrow conditions. In this case, increased diversity of visual sensitivities would be expected in broadband environments, given that multiple wavelengths can be matched by phenotypes (McFarland and Munz 1975b). In contrast, spectrally narrow photic conditions should limit the evolution of phenotypes around one single “sensitivity optimum”. While phenotypic evolution might be easier to predict when a reduced number of phenotypes are clearly favored, multiple simultaneous selective pressures might obscure determinism in variable heterogeneous environments (Bell 2010; Nosil et al. 2018; Reimchen and Bergstrom 2023).

Here, we investigate the role of photic environments as drivers of phenotypic evolution in visual sensitivities along a photic gradient placed within a natural experiment. For this, we measured the difference in photic conditions between great and crater lakes and determined the divergence in visual sensitivity between pairs of source and derived populations of wild-caught and laboratory-reared Midas cichlid fish (*Amphilophus* cf. *citrinellus*) to test the following hypotheses: (1) phenotypic changes in the visual system of Midas cichlids are in the same direction as changes in photic conditions and thus potentially adaptive, (2) the degree of phenotypic change is correlated with the degree of environmental change, and (3) most of the variation in visual sensitivity can be explained by the photic conditions at the lake of origin rather than by rearing condition (i.e., there is a strong genetic component). Overall, we provide evidence that visual sensitivities vary continuously by finetuning the expression of opsin genes and that their evolution is consistent with the sensitivity hypothesis. We show that while visual sensitivities match photic conditions in a predictable manner, their phenotypic range within a given habitat is influenced by environment-specific selection regimes, with spectrally narrow habitats exhibiting reduced intrapopulation phenotypic variation.

## Materials and methods

### *Study Design*

In Nicaragua, a natural experiment occurred, where from a common source population in the great lakes Managua and Nicaragua, seven isolated crater lakes were independently colonized by Midas cichlid fish (*Amphilophus* cf. *citrinellus*) between 4,700 to 800 years ago (Barluenga et al. 2006; Kautt et al. 2016; 2020). The young radiation of Midas cichlids currently encompasses 13 nominal species characterized by genomic and morphological differentiation among lakes with sympatric and allopatric species showing divergence in traits related to lip size, body shape, pharyngeal morphology, or body coloration (Fig 1A, Torres-Dowdall and Meyer 2021). Given the isolated nature of the crater lakes, their colonization from common source populations

and their geomorphological similarities, crater lakes have been considered as natural replicates regarding many of their environmental factors (Kautt et al. 2018). However, photic conditions differ widely among Nicaraguan lakes. The great lakes are big and shallow and the winds create waves that constantly stir up the sediments making them very turbid (Elmer et al. 2010). Similar light conditions can be found in the San Juan River, a major river connected to Lake Nicaragua that is also inhabited by Midas cichlids. In contrast, the crater lakes are very deep and thus sediments are deposited at depths far from the influence of waves which might contribute to the observation that most crater lakes are clearer than the great lakes, but there is still substantial variation among crater lakes (Torres-Dowdall and Meyer 2021). Studies on the visual ecology of the two oldest crater lakes Apoyo and Xiloá found convergent changes in the visual system of these populations regardless of their color morphs suggesting a strong effect of the ambient light environment (Härer et al. 2018; Torres-Dowdall et al. 2017). However, given the diversity of photic environments found among crater lakes, their population isolation (i.e., absence of gene flow), and their recent and independent colonization from a common source, the system provides an excellent opportunity to investigate the predictability of phenotypic evolution in visual systems along a wide range of photic conditions by asking, how closely do visual systems track local conditions along a natural gradient?

### *Characterization of the Photic Environments*

To characterize the photic conditions found among the Nicaraguan lakes, underwater irradiance was measured from both great lakes, Managua and Nicaragua, seven neighboring crater lakes, and one riverine population (Fig. 1B) Absolute irradiance was measured using a spectrometer (FLAME-S-XR1-ES, Ocean Insight, USA) connected to a 25-m UV-VIS optical fiber (OCF-104472, Ocean Insight, USA) with a cosine corrector (CC-3-UV-S, Ocean Insight, USA). Multiple consecutive measurements during daytime between 10 am-2 pm were performed at 0.15 m, 1 m, 3 m, 5 m, 10 m, 15 m, 20 m, and 25 m depth. Sites with less than 25 m depth were measured



until their deepest point. The measurements were performed by orienting the sensor upwards (downwelling irradiance,  $E_d$ ), sideways (sidewelling irradiance,  $E_s$ ), and downwards (upwelling irradiance,  $E_u$ ). Absolute irradiance measurements were corrected for integration time and converted to photons/cm<sup>2</sup>/s/nm ( $E$ ) based on Johnsen (2012) follows:

$$E = W(\lambda) \left( \frac{1}{h * c} \right) \quad (1)$$

where  $W$  represents the irradiance in energy units as W/m<sup>2</sup>/nm at each wavelength  $\lambda$ ,  $h$  represents Planck's constant in m<sup>2</sup>\*kg/s and  $c$  the speed of light in m/s. To minimize the effect of outliers due to handling of the spectrometer, median absolute irradiance of 3-10 measurements for each depth was used and smoothed using a rolling mean over 5 nm following the manufacturer's instructions (oceaninsight.com; Fig. S1). Only wavelengths within the visible spectrum (350-700 nm) were used based on the peak sensitivity of visual pigments in fish (Carleton et al. 2020; Rennison et al. 2016). To allow the comparison of spectral shape across sites, absolute spectra were divided by their respective maximal value resulting in normalized irradiance (Fig. 1B).

### *Opsin Gene Expression*

To determine the degree of variation in cone opsin expression in populations of Midas cichlids, six to eight wild-caught adult fish per site were collected in January and February 2018 from ten locations across Nicaragua for a total of 78 individuals (Table S1). In the rest of the text, the term "population" is used to refer to this level of sampling (i.e., locations), although some of the sampled populations correspond to formally described species within the Midas cichlid radiation. Additionally, 62 lab-reared adults from nine populations raised for at least two generations in the animal research facility at the University of Konstanz were included in our study. These laboratory experiments were done to measure phenotypic variability in the absence of developmental noise due to the different light conditions fish experience in the wild. Only sexually mature fish (at least

2 years old) were used given that opsin gene expression varies during ontogeny eventually reaching a developmental plateau at adulthood (Härer et al. 2017; 2019). Fish were sampled during the same daytime (11am-3pm) to control for diurnal variation in gene expression (Yourick et al. 2019), and euthanized by applying an overdose of MS-222 and subsequent cervical dislocation. The retinas were removed and stored in RNAlater (Sigma-Aldrich, USA) at -20°C until extraction. RNA was extracted using a standard Trizol-chloroform protocol based on Rio et al. (2010). For each sample, 200 ng of total RNA were used to synthesize first-strand cDNA using the manufacturer's protocol (GoScript™ Reverse Transcription System, Promega, USA). Gene expression of six cone opsin genes (*sws1*, *sws2b*, *sws2a*, *rh2aβ*, *rh2b* and *lws*) and two reference genes (*gapdh* and *imp2*) was measured using quantitative real-time PCR (qPCR) for 40 cycles (CFX96™, Bio-Rad Laboratories, USA) following Härer et al. (2017). Expression of the paralog *rh2aα* was not measured since it is not expressed in Midas cichlids (Torres-Dowdall et al. 2017). Mean threshold cycle (Ct) values from three technical replicates were used for analysis. Primer sequences, amplification efficiencies, and mean expression of reference genes are reported in the supplementary material (Table S2-S3, Fig S3). Proportional opsin expression for each individual was calculated as the amount of each cone opsin ( $T_i$ ) relative to the total cone opsin expression ( $T_{all}$ ) as Fuller et al. (2004):

$$\frac{T_i}{T_{all}} = \frac{(1/((1+E_i)^{Ct_i}))}{\sum(1/((1+E_i)^{Ct_i}))} \quad (2)$$

where  $E_i$  is the efficiency of primer  $i$ ,  $Ct_i$  the critical cycle number for gene  $i$ , and the overall sum of the proportional expressions of the six opsin genes equals one. To test for divergence among lakes due to photic conditions, opsin expression was analyzed using ANOVA (type II) with lake of origin as the predictor variable and proportional opsin expression as the response variable. When significant, pairwise comparisons were analyzed using Tukey's HSD post hoc test.

### *Testing the Association between Photic Changes and Sensitivity Shifts*

To determine if changes in the visual system between ancestral and derived populations are correlated with differences in the photic conditions between the source and the derived habitats, we took advantage of our knowledge about the demographic history of Midas cichlids (Kautt et al. 2020). Extensive population genomic analyses showed that Crater Lake Apoyo was colonized from Great Lake Nicaragua and all other crater lakes from Great Lake Managua. While the ancestry of Crater Lake Masaya is admixed, Great Lake Managua is considered its main population source for analysis in this study due to the small contribution of Great Lake Nicaragua (~22%, Kautt et al. 2018; 2020). We asked if photic habitat differences drive the phenotypic divergence seen between source and derived populations of Midas cichlids. For this, we calculated the degree of correlation between spectral attenuation coefficients ( $K_d$ ) and estimated spectral sensitivity curves ( $\Delta SSC_j$ ). Spectral attenuation coefficients represent the extinction of ambient downwelling light with depth and are less prone to background noise (e.g., atmospheric events, waves) than irradiance, making it a more robust estimate of the spectral characteristics of water bodies (Mobley 1994; Rennison et al. 2016). The localized spectral attenuation coefficient,  $K_d$ , was calculated based on Sabbah et al. (2011) as follows:

$$K_d(\lambda) = \frac{1}{z} \ln[E_{d,z}(\lambda) - E_{d,0}(\lambda)] \quad (3)$$

where  $E_{d,z}$  is the downwelling irradiance at depth  $z$  (one meter in this study) and  $E_{d,0}$  the downwelling irradiance 15 cm below the water surface for each wavelength  $\lambda$  ranging from 350-750 nm (Fig. S4). Next, we determined the change in predicted visual sensitivity experienced by fish from derived populations compared to the source populations. For this, the individual continuous estimates of visual sensitivity, the spectral sensitivity curves ( $SSC_j$ ) were estimated for each specimen following Rennison et al. (2016). In short, absorbance templates from Govardovskii et al. (2000) and absorption peaks from Torres-Dowdall et al. (2017) for each opsin were used. We simulated scenarios assuming either only A<sub>1</sub>- or only A<sub>2</sub>- chromophore usage. The

sensitivity curve was then weighted by the proportional expression of each opsin and the sensitivity curves of the six expressed opsins were added (Fig. S5). Subsequently, shifts in spectral sensitivity curves ( $\Delta SSC_j$ ) were estimated as the difference between the median spectral sensitivity of the source population and the individual spectral sensitivities of each fish in the derived populations as in Rennison et al. (2016):

$$\Delta SSC_j(\lambda) = [\tilde{x}_s(\lambda)]_{Source} - [SSC_j(\lambda)]_{Derived} \quad (4)$$

where  $SSC_j$  is the individual spectral sensitivity curve. Finally, we ran Pearson's correlation tests between shifts in spectral sensitivity ( $\Delta SSC_j$ ) and changes in attenuation coefficients ( $\Delta K_d$ ) for each individual. Similar analyses but using changes in spectral irradiance ( $\Delta E_d$ ) instead of  $\Delta K_d$  are reported in the supplementary material (Fig. S6). All  $p$ -values were corrected for multiple testing using the Benjamini-Hochberg FDR method (Benjamini and Hochberg 1995). All statistical analyses were performed in R (R Core Team 2020).

### *Predictability of Visual Sensitivity based on Photic Conditions*

To test if the spectral sensitivity of fish can be predicted based on their local photic conditions, we used point estimates for visual sensitivity and regressed on a composite axis of the photic conditions at their lake of origin at one meter depth. One meter depth was chosen as a compromise to include all sites (shallow habitats ~2m depth) and in agreement with the habitat ecology of Midas cichlids (Dittmann et al. 2012; Oldfield et al. 2006). The composite axis was generated using correlation-based principal components analysis (PCA) of seven z-standardized variables. We used down- and sidewelling  $\lambda P_{50}$  as the spectrum-halving wavelength which summarizes the photon distribution into a single value indicating short- or long-wavelength predominant spectra (McFarland and Munz 1975a). We also included  $\lambda P_{25}$  and  $\lambda P_{75}$ , the wavelengths within which 50% of the photons are found (i.e., spectral broadness). Finally, the percentage of downwelling photons available at one meter compared to 15 cm below the water

surface, an estimate of luminosity % $E_d$ , was also included in the PCA (Table S4). The response variable predicted sensitivity index (PSI) was defined as the sum of peaks in absorption of each opsin weighted by its proportional expression in the retina (Hofmann et al. 2009) and calculated using the following equation:

$$PSI_j = PE_{sws1} \times 360 \text{ nm} + PE_{sws2b} \times 440 \text{ nm} + PE_{sws2a} \times 466 \text{ nm} + PE_{rh2b} \times 500 \text{ nm} + PE_{rh2a\beta} \times 555 \text{ nm} + PE_{lws} \times 610 \text{ nm} \quad (5)$$

where  $PE$  is the proportional cone opsin expression for each individual using opsin absorbance peaks assuming  $A_2$ -chromopore usage from Torres-Dowdall et al. (2017).

To determine the genetic component of the phenotypic variation found in the visual system of Midas cichlids, we also estimated the predicted sensitivity index of individuals reared in the laboratory. Given that phenotypic divergence in the wild could also be mediated by environmentally induced changes, phenotypic variation measured under common-garden conditions informs about its genetic component. We used a linear mixed-effect model to determine the percentage of phenotypic variation that is explained by native photic conditions independently of rearing conditions. The model considered the predicted sensitivity index (PSI) as the response variable, photic environment (PC1), rearing environment (i.e., wild or lab), and their interaction as predictor variables (fixed effects); lake of origin was used as a random intercept. The relative importance of each regressor to the amount of explained variance was estimated based on Stoffel et al. (2021). Confidence intervals for mean regression lines accounting for standard error of the regression line and intercept on each population were calculated following Breheny and Burchett (2017). To account for potential bias in predicting spectral sensitivity from gene expression data, a sensitivity analysis to assess robustness of predictors and outcome to unobserved confounding factors was performed as in Cinelli and Hazlett (2020). Additionally, we regressed the coefficients of variation in our estimates of visual sensitivity (PSI) within each

population against the photic axis (PC1) to test if phenotypic variation is reduced in spectrally narrow environments. Diagnostic plots are provided in the supplemental materials (Fig. S10-11).

## Results

### *The Photic Gradient Along the Nicaraguan Great and Crater Lakes*

The photic gradient of the Nicaraguan lakes consists of a composite axis that ranges from broad, short wavelength-shifted, and bright crater lakes up to narrow, long wavelength-shifted, and dim great lakes (Fig.1, Table S4). The principal component analysis including all photic parameters at 1m depth identified one main axis explaining most of the variation (PC1= 93%) and was mainly driven by photon distribution of both down- and sidewelling irradiance (Fig. S7). In contrast, PC2 explained only 4.86% of the variance in photic conditions and was mainly driven by relative downwelling luminosity (Table S4). Within the photic gradient (e.g., PC1), Crater Lake Apoyo represents the most blue-shifted environment followed by crater lakes As. Managua, Apoyeque and Xiloá. Crater lakes As. León and Masaya represent intermediate lakes within the photic gradient (PC1). Crater Lake Tiscapa has extremely low luminosity values but shows similar spectral properties as Great Lake Nicaragua and River San Juan. Great Lake Managua represents the most red-shifted environment (Table S4, Fig. S7). The presence of phototropic microorganisms, specifically cyanobacteria and green algae (Stomp et al. 2007), contributes to the spectral peaks around 640 and 700 nm seen in some lakes (i.e., Tiscapa and Managua, Fig. 1B, S2).

### *Opsin Gene Expression varies significantly across Nicaraguan lakes*

We found significant variation in opsin gene expression in wild-caught individuals where, for at least one opsin gene, all derived crater lakes populations show divergence from the source great lakes (Fig. 2). Fish from short wavelength-shifted lakes tend to express more *sws2b* and *rh2a* (and less *sws2a* and *lws*) in single and double cones respectively. These patterns of opsin gene

expression were also observed in individuals from the different lakes reared under common garden conditions, which suggests a strong genetic component. Although the laboratory-reared fish experienced the same photic conditions during development, the distinct populations still showed significant variation in opsin gene expression for most opsins (Fig. S8).

*Shifts in spectral sensitivity are correlated with changes in photic conditions following colonization events*

Our results show that spectral sensitivities from the source populations in the great lakes have shifted in the same direction as the changes in photic conditions, suggesting the repeated and independent evolution of visual sensitivity in all seven crater lake populations. Based on the known colonization history of Midas cichlids across the Nicaraguan lakes (Kautt et al. 2020), we asked whether the modulation in opsin expression across lakes resulted in changes in visual sensitivity that correlate with the changes in photic conditions (spectral attenuation coefficients,  $K_d$ ) fish experienced after colonizing the crater lakes (Figs. S4-S5). Coefficients were significantly positively correlated averaging  $0.53 \pm 0.01$  and  $0.65 \pm 0.01$  (mean $\pm$ SE) assuming A<sub>1</sub>- and A<sub>2</sub>-chromophore usage respectively (Fig. 3). These results were sustained, although weakened, when irradiance was used as a measure of the photic environment rather than  $K_d$  (Fig. S6).

*Spectral sensitivity of Midas cichlids is predicted by photic conditions at their lake of origin*

If variation in the visual system is driven by the light environment, differences in visual sensitivity among populations should be most strongly predicted by their native photic conditions. We tested this, by using a linear mixed-effect model with PC1, the main environmental composite axis of photic conditions (Table S4, Fig. S8), as an explanatory variable for the variation in the predicted sensitivity index (PSI, Fig. 4A). The fixed effects in our model explained on average about 64% of the overall variation in predicted sensitivity index (PSI) with 51-74% confidence interval (CI) based on 1000 parametric bootstrapping iterations (Fig. S9). About 48% of the variation in visual

sensitivity of Midas cichlids across populations was explained by the photic environment in their native habitat (34-62% CI, Fig. S9). We also found that the visual sensitivity of fish varies depending on rearing conditions (e.g., wild-caught or lab-reared), demonstrating that there is an environmental component that explains on average 13% of the overall variance (0-33% CI, Fig. S9). There is a non-significant interaction ( $F_{(1,130,0.75)}=3.407$ ,  $p=0.067$ ) between the native photic environment and rearing conditions, which explained less than 1% of the variation in PSI (0-22%, Fig. S9). Further, sensitivity analysis reveals that confounding factors accounting for less than 54% of the residual variance of both photic conditions and predicted sensitivity would not suffice to deem the estimates as statistically not significant ( $RV_{q=1,\alpha=0.05}=54.9\%$ , Table S6). This implies that even confounders that explain all the residual variation of the outcome and as strong as the rearing effect are not sufficient to override the effect of the photic environment in our model and thus our conclusions (i.e.,  $R^2_{Y\sim Z|X,D} < R^2_{Y\sim D|X}$ ; Table S5). Additionally, we tested if variation in PSI within each population changed in response to the photic conditions, specifically that spectrally broad environments show higher variation in predicted sensitivity indexes than narrow ones. Our results show that coefficients of variation in PSI are significantly affected by photic conditions (PC1) in wild-caught fish (Fig 4A,  $F_{(1,8)}=13.25$ ,  $p= 0.0066$ ), but not in laboratory-reared fish ( $F_{(1,7)}=2.47$ ,  $p= 0.16$ ). According to our results, most of the variation in visual sensitivity seen across populations of Midas cichlids along the photic gradient has a strong genetic component and a relatively smaller environmental effect (Fig 4A). Further, the phenotypic range of visual sensitivities within each population is clearly shaped by ambient photic conditions, with decreasing diversity as environments become more spectrally restricted (Fig 4B).

## Discussion

The visual sensitivity of fishes often varies across light environments and this variation is commonly interpreted as adaptive (reviewed in Carleton et al. 2010; Carleton and Yourick 2020; Musilova et al. 2021). Most studies in visual ecology have focused on comparisons between



strongly contrasting habitats such as marine vs freshwater (Rennison et al. 2016), shallow vs deep-water (Sugawara et al. 2005) or stained/turbid vs clear waters (Fuller et al. 2004; Torres-Dowdall et al. 2017). By analyzing the photic environments in a dichotomous manner, these studies maximize the power to identify adaptive patterns in the visual system. However, fishes inhabit a wide range of conditions that need to be considered to fully understand the diversity of visual systems seen across natural populations (Flamarique et al. 2013; Kirk 2010; Sabbah et al. 2011). By focusing on how visual sensitivities vary in response to a gradient in photic conditions, this study is able to determine aspects about the evolution of visual systems that were not evident by simply comparing the ends of these gradients (Torres-Dowdall et al. 2017). Below, we discuss how studying variation in the visual system of closely related species living under a wide range of photic conditions allows the identification of links between genotype, phenotype and fitness, providing novel insights into the mechanisms and pace of adaptive evolution.

The predictability of evolutionary outcomes depends on multiple factors such as the strength of natural selection or the time scale over which evolutionary changes are observed (Grant and Grant 2002; Reimchen and Bergstrom 2023). Strong selective pressures due to colonization of novel habitats might determine the direction of evolution over short periods of time. However, many other factors influence evolutionary outcomes and often hinder the predictability of long-term evolutionary trajectories (Bell 2010; Nosil et al. 2018). Hence, when repeated or convergent evolution of phenotypes is observed, it is often considered a signature of determinism in the evolutionary responses of organisms to common environmental pressures (Blount et al. 2018; Losos 2018). Here, we show that the visual systems of all seven derived crater lake populations have repeatedly shifted their visual sensitivity in a predictable manner, reflecting changes in photic conditions. Our study highlights the role of the photic environment imposing selection on the visual system, driving predictable phenotypic evolution of visual sensitivities along an environmental gradient in the absence of gene flow.

While there is a predictable change in phenotypes along the photic gradient, the phenotypic range observed within populations suggests a more complex scenario. Understanding how phenotypic variation is maintained in the wild requires information about the fitness consequences of environmental pressures, which can be visualized as fitness landscapes (Wright 1932). While the relative fitness of certain phenotypes is often unknown, the distribution of phenotypes within a population can inform about the shape of the selective landscape (Svensson 2023). For instance, habitats with single steep adaptive peaks might select for a modal phenotype, whereas broad, “flat” selective landscapes should allow for multiple phenotypes of similar fitness (Reimchen and Bergstrom 2023). Our data suggests that selective landscapes vary along the photic gradient, becoming less defined around a single modal phenotype as the environment becomes more spectrally heterogeneous. Spectrally broader environments may exert weaker selective pressures, allowing the emergence of distinct visual sensitivities that may be selected for by other factors (e.g., diet, mate choice, microhabitat). This is expected to reduce predictability based solely on photic conditions. In contrast, as turbidity increases, the spectral range is narrowed and luminosity reduced, with fewer remaining photons being distributed among fewer wavelengths. Those spectrally narrow habitats seem to select for reduced variation in visual sensitivity around a modal phenotype tuned to the specific spectral range available (e.g., Fig. 4A).

The photic gradient along the Nicaraguan lakes is best represented as a composite axis that ranges from the clearest, short-wavelength shifted, spectrally broad, and relatively bright Crater Lake Apoyo up to the most turbid, longwave-shifted, spectrally narrow, and dim Great Lake Managua. In this regard, the strong associations between changes in visual sensitivity and photic habitat seen when comparing ancestral and derived populations of Midas cichlids suggest that their visual systems are locally adapted (Fig. 3). Using this same approach, Rennison et al. (2016) identified patterns of rapid adaptive evolution in the visual system of freshwater vs marine threespine stickleback, *Gasterosteus aculeatus*. However, the habitats compared in that study

represented rather clear aquatic habitats. This contrasts with some of the drastic differences in photic conditions between crater lakes and great lakes seen in our study, which could enhance our power to detect significant correlations between opsin gene expression and photic changes. Alternatively, if our findings that broad-spectrum environments facilitate the emergence of multiple visual sensitivities of similar fitness are generalizable to other systems (Carleton et al. 2016; Loew 1995; Reimchen and Bergstrom 2023; Schneider et al. 2020), this could also help explain the greater intrapopulation variation found in Rennison et al. (2016) compared to this study. The narrower spectra of some of the Nicaraguan lakes might select for sensitivities tuned to the specific spectral band available, resulting in stronger correlations between habitat conditions and visual sensitivity (Bowmaker 1990). Hence, our ability to predict phenotypic change, a major goal in biology, especially in the context of environmental perturbations to aquatic ecosystems (Bunnell et al. 2021; Seehausen et al. 1997; Solomon et al. 2015), might depend on both the magnitude of the environmental change and the narrowness of the adaptive peak.

Even in the presence of strong, deterministic selective pressures, phenotypic evolution might not occur as predicted. Adaptive evolution requires heritable traits to be selected over multiple generations to “optimize” phenotypes, while phenotypic plasticity could also tune phenotypic variation within an organism’s lifetime (Fisher 1930). Thus, understanding both genetic and plastic contributions to phenotypic variation is critical for assessing the likelihood and speed of adaptive evolution (Ghalambor et al. 2007; Hendry and Kinnison 1999). Given the correlated changes in visual sensitivity of Midas cichlids in response to the colonization of crater lakes, we asked how closely these independent populations tracked the observed gradient in photic conditions. Our model including rearing conditions (wild vs. common garden) and photic conditions at lake of origin explained 64% of the variation found in visual sensitivity (Fig. 4A). Overall, 48% of the variation was explained by the photic conditions in the lake of origin, suggesting a strong genetic component. Although photic conditions have a strong power to

explain phenotypic variation in visual sensitivity of Midas cichlids, there is still some unexplained variation that could arise from other factors proposed in the literature (e.g., diet, mate choice; Carleton and Yourick 2020), which may be particularly important in clear lakes. Among others, spectral tuning in cichlid vision has been associated with foraging habits (Hofmann et al. 2009; Irisarri et al. 2018), mate choice (Schneider et al. 2020; Seehausen et al. 2008), or ecological and lineage-specific factors (Schott et al. 2014; Torres-Dowdall et al. 2015). However, the 13 described species in the small Midas cichlid radiation overlap in their dietary requirements and show almost no sexual dimorphism in coloration (Fig. 1A, Torres-Dowdall and Meyer 2021), supporting the conclusion that these factors may only be minor drivers of visual divergence in our system. Further, while adaptive evolution appears to be the main driver of phenotypic variation, the role of plasticity in the visual system must also be considered. Even when plasticity is incomplete and thus not sufficient for organisms to reach certain adaptive peaks (Fisher 1930; Ghalambor et al. 2007), it might facilitate the emergence and maintenance of variation within populations, particularly in spatially and temporally heterogeneous environments (Pigliucci 2001). For instance, reductions in water clarity have been reported in our system due to algal blooms (e.g., As. Managua; Torres-Dowdall et al. 2014) or modern anthropogenic pollution (e.g., Tiscapa; García Espinoza 2020). In theory, changes in water clarity should have the strongest visual repercussions in clear environments (Kirk 2010; Lythgoe 1979; Mobley 1994). This may explain the increased variation in visual sensitivity observed in broadband environments (Fig. 4b), as spatial or temporal heterogeneity could allow multiple sensitivity phenotypes to be adaptive and/or favor plasticity (Fuller and Claricoates 2011; Härer et al. 2017).

Given the known demographic history of Midas cichlids (Kautt et al. 2016; 2020), which rules out the possibility of crater lake to crater lake dispersal and thus any gene flow between crater lakes, we were able to estimate evolutionary rates for all derived populations (0.0009-0.0121 Haldanes, Table S5) highlighting that phenotypic evolution has occurred rapidly and

independently in all seven newly colonized crater lakes (see Hendry and Kinnison 1999 for comparison). The most common shifts in visual sensitivity among Midas cichlid species are achieved by modulating the expression of the three most abundant opsins, namely *sws2a* in single cones, and *rh2a* and *lws* in double cones (Fig. 2). Overall, this suggests that by modulating the relative expression of opsin genes, phenotypic variation in visual sensitivity can be gradually tuned across populations (Veen et al. 2017). However, populations such as Crater Lake Apoyo show conditional expression of additional opsins (Fig. S8). Interestingly, the gradual phenotypic variation observed across populations seems to be achieved by two non-exclusive mechanisms, namely the conditional expression of different genes (e.g., *sws2b* paralog in Apoyo) and the quantitative regulation of the predominantly expressed cone opsin genes (i.e., *sws2a*, *rh2a*, *lws*). The phenotypic variation in Midas cichlids along the photic gradient suggests that visual sensitivity in these fish is a continuous trait, rather than discrete phenotypes compartmentalized into palettes (Fig. 4).

Overall, we documented compelling evidence that selection pressures imposed by light environments have resulted in rapid phenotypic divergence in the visual system of Midas cichlids. In the source populations inhabiting turbid great lakes with low light availability and narrow spectral conditions, fine-tuning visual sensitivity to maximize photon catch resulted in little phenotypic variation around a modal phenotype. As fish began to colonize the newly formed crater lakes, they encountered a variety of photic conditions. Here, Midas cichlids repeatedly and predictably adjusted their visual sensitivity as they encountered these novel habitats, as evidenced by the changes in spectral sensitivity positively correlating with photic changes (Fig. 3). Our results further suggest that predictability might depend not only on the organisms, but also on the environment itself, as less selective environments might result in a wider array of potentially equally well adapted phenotypes (Nosil et al. 2018; Reimchen and Bergstrom 2023). Accordingly, in spectrally broader environments, weaker selection towards a modal phenotype also allowed

for more variable phenotypes to emerge. The evolutionary history of the Midas cichlid visual system relied on the modulatory expression of visual opsin genes to generate tuned sensitivities. The change in visual sensitivity was mainly driven by rapid phenotypic evolution rather than plasticity, as the phenotypic variation in the Midas cichlid visual system shows a strong heritable component inferred from individuals reared under common garden (Fig. 4A). In conclusion, the repeated divergence of visual sensitivities among crater lake populations of Midas cichlids by modulating their expression of cone opsin genes provides an evolutionary lesson on the mechanisms and reasons that facilitate phenotypic variation closely tracking environmental conditions.

## **Acknowledgments**

We would like to thank current and previous members of the Meyer lab, particularly to Femina Prabhukumar for helping with qPCR experiments, and Sina J. Rometsch for reviewing an early version of this manuscript. We thank Diana J. Rennison for sharing the code to analyze spectral data and Ad Konings for kindly providing photographic material. We thank the Nicaraguan Ministerio del Ambiente y los Recursos Naturales (MARENA) for granting permits for fieldwork and specimen collection. We thank two anonymous reviewers for their helpful comments. Laboratory-reared fish were sacrificed under permit T-16/13 from the Animal Research Facility of the University of Konstanz. This work was mainly supported by grants from the Deutsche Forschungsgemeinschaft (DFG, grant number TO 914/3-1) to J.T.D. and A.M., the Young Scholar Fund of the University of Konstanz (grant number FP 794/15) to J.T.D., and a European Research Council Advanced Grant (ERC, grant number 293700-GenAdapt) to A.M.

The authors declare no conflict of interest.

## Statement of Authorship

J.T.D., A.H., and A.M. developed the original project and performed the fieldwork; J.T.D., N.K., and C.B. reared fish and dissected the lab specimens; J.T.D. and A.M coordinated the experiments and supervised the project; C.B., A.H., J.T.D, and N.K., collected the data; C.B. analyzed the data and led the writing of the manuscript. All authors contributed critically to the draft and gave final approval for publication.

## Data Availability Statement

Data and code associated with this study are publicly available on Dryad data repository [doi.org/10.5061/dryad.j3tx95xgk](https://doi.org/10.5061/dryad.j3tx95xgk) (Bertinetti et al. 2023).

## Literature Cited

- Baden, T. 2021. Circuit mechanisms for colour vision in zebrafish. *Current Biology* 31:R807-R820.
- Baden, T., and D. Osorio. 2019. The Retinal Basis of Vertebrate Color Vision. *Annual Review of Vision Science* 5:177-200.
- Barluenga, M., K. N. Stölting, W. Salzburger, M. Muschick, and A. Meyer. 2006. Sympatric speciation in Nicaraguan crater lake cichlid fish. *Nature* 439:719-723.
- Barrett, R. D., S. M. Rogers, and D. Schluter. 2008. Natural Selection on a Major Armor Gene in Threespine Stickleback. *Science* 322:255-257.
- Bayliss, L., R. J. Lythgoe, and K. Tansley. 1936. Some new forms of visual purple found in sea fishes with a note on the visual cells of origin. *Proceedings of the Royal Society B* 120:95-113.
- Becker, U., G. Colling, P. Dostal, A. Jakobsson, and D. Matthies. 2006. Local adaptation in the monocarpic perennial *Carlina vulgaris* at different spatial scales across Europe. *Oecologia* 150:506-518.

- Bell, G. 2010. Fluctuating selection: the perpetual renewal of adaptation in variable environments. *Philosophical Transactions of the Royal Society B* 365:87-97.
- Benjamini, Y., and Y. Hochberg. 1995. Controlling the false discovery rate: a practical and powerful approach to multiple testing. *Journal of the Royal Statistical Society: Series B (Statistical Methodology)* 57:289-300.
- Bertinetti, C., A. Härer, N. Karagic, A. Meyer, and J. Torres-Dowdall. 2023. Data from: Repeated Divergence in Opsin Genes Expression Mirrors Photic Habitat Changes in Rapidly Evolving Crater Lake Cichlid Fishes. *American Naturalist*, Dryad Digital Repository, <https://doi.org/10.5061/dryad.j3tx95xgk>.
- Bishop, J. A. 1972. An Experimental Study of the Cline of Industrial Melanism in *Biston betularia* (L.) (Lepidoptera) between Urban Liverpool and Rural North Wales. *Journal of Animal Ecology* 41:209.
- Blount, Z. D., R. E. Lenski, and J. B. Losos. 2018. Contingency and determinism in evolution: Replaying life's tape. *Science* 362:eaam5979.
- Bowmaker, J. K. 1990. Visual pigments of fishes, Pages 81-107 in R. Douglas, and M. Djamgoz, eds. *The Visual System of Fish*. Dordrecht, Springer Netherlands.
- Breheny, P., and W. Burchett. 2017. Visualization of regression models using visreg. *R J.* 9:56.
- Bunnell, D. B., S. A. Ludsin, R. L. Knight, L. G. Rudstam, C. E. Williamson, T. O. Höök, P. D. Collingsworth et al. 2021. Consequences of changing water clarity on the fish and fisheries of the Laurentian Great Lakes. *Canadian Journal of Fisheries and Aquatic Sciences* 78:1524-1542.
- Carleton, K. L., B. E. Dalton, D. Escobar-Camacho, and S. P. Nandamuri. 2016. Proximate and ultimate causes of variable visual sensitivities: Insights from cichlid fish radiations. *Genesis* 54:299-325.



- Carleton, K. L., D. Escobar-Camacho, S. M. Stieb, F. Cortesi, and N. J. Marshall. 2020. Seeing the rainbow: mechanisms underlying spectral sensitivity in teleost fishes. *Journal of Experimental Biology* 223.
- Carleton, K. L., C. M. Hofmann, C. Klisz, Z. Patel, L. M. Chircus, L. H. Simenauer, N. Soodoo et al. 2010. Genetic basis of differential opsin gene expression in cichlid fishes. *Journal of Evolutionary Biology* 23:840-853.
- Carleton, K. L., and M. R. Yourick. 2020. Axes of visual adaptation in the ecologically diverse family Cichlidae. *Seminars in Cell & Developmental Biology* 106:43-52.
- Cinelli, C., and C. Hazlett. 2020. Making Sense of Sensitivity: Extending Omitted Variable Bias. *Journal of the Royal Statistical Society Series B: Statistical Methodology* 82:39-67.
- Clarke, G. L. 1936. On the depth at which fish can see. *Ecology* 17:452-456.
- Clausen, J., D. D. Keck, and W. M. Hiesey. 1948. Environmental responses of climatic races of *Achillea*. *Experimental studies on the nature of species*. III.
- Crescitelli, F., M. McFall-Ngai, and J. Horwitz. 1985. The visual pigment sensitivity hypothesis: further evidence from fishes of varying habitats. *Journal of Comparative Physiology A* 157:323-333.
- Cronin, T. W., and M. J. Bok. 2016. Photoreception and vision in the ultraviolet. *Journal of Experimental Biology* 219:2790-2801.
- Cronin, T. W., S. Johnsen, N. J. Marshall, and E. J. Warrant. 2014. *Visual ecology*, Princeton University Press.
- Davies, W. I., S. P. Collin, and D. M. Hunt. 2012. Molecular ecology and adaptation of visual photopigments in craniates. *Molecular Ecology* 21:3121-3158.
- Dittmann, M. T., M. Roesti, A. Indermaur, M. Colombo, M. Gschwind, I. Keller, R. Kovac et al. 2012. Depth-dependent abundance of Midas Cichlid fish (*Amphilophus* spp.) in two Nicaraguan crater lakes. *Hydrobiologia* 686:277-285.

- Elmer, K. R., H. Kusche, T. K. Lehtonen, and A. Meyer. 2010. Local variation and parallel evolution: morphological and genetic diversity across a species complex of neotropical crater lake cichlid fishes. *Philosophical Transactions of the Royal Society B* 365:1763-1782.
- Endler, J. A. 1977, *Geographic Variation, Speciation and Cline*, Princeton University Press.
- Endler, J. A. 1986, *Natural selection in the wild*, Princeton University Press.
- Filchak, K. E., J. B. Roethele, and J. L. Feder. 2000. Natural selection and sympatric divergence in the apple maggot *Rhagoletis pomonella*. *Nature* 407:739-742.
- Fisher, R. A. 1930, *The Genetical Theory of Natural Selection*, The Clarendon Press.
- Flamarique, I. N., C. L. Cheng, C. Bergstrom, and T. E. Reimchen. 2013. Pronounced heritable variation and limited phenotypic plasticity in visual pigments and opsin expression of threespine stickleback photoreceptors. *Journal of Experimental Biology* 216:656-667.
- Fuller, R. C., K. L. Carleton, J. M. Fadool, T. C. Spady, and J. Travis. 2004. Population variation in opsin expression in the bluefin killifish, *Lucania goodei*: a real-time PCR study. *Journal of Comparative Physiology. A: Neuroethology, Sensory, Neural, and Behavioral Physiology* 190:147-154.
- Fuller, R. C., and K. M. Claricoates. 2011. Rapid light-induced shifts in opsin expression: finding new opsins, discerning mechanisms of change, and implications for visual sensitivity. *Molecular Ecology* 20:3321-3335.
- García Espinoza, M. 2020. Estudio sobre el impacto ambiental antrópico en la laguna de Tiscapa, Managua. *Raíces: Revista Nicaragüense de Antropología*:90-104.
- García-Ramos, G., and M. Kirkpatrick. 1997. Genetic Models of Adaptation and Gene Flow in Peripheral Populations. *Evolution* 51:21-28.
- Ghalambor, C. K., J. K. McKay, S. P. Carroll, and D. N. Reznick. 2007. Adaptive versus non-adaptive phenotypic plasticity and the potential for contemporary adaptation in new environments. *Functional Ecology* 21:394-407.

- Girvan, J. R., and V. A. Braithwaite. 1998. Population differences in spatial learning in three-spined sticklebacks. *Proceedings of the Royal Society B* 265:913-918.
- Govardovskii, V. I., N. Fyhrquist, T. O. M. Reuter, D. G. Kuzmin, and K. Donner. 2000. In search of the visual pigment template. *Visual Neuroscience* 17:509-528.
- Grant, P. R., and B. R. Grant. 2002. Unpredictable Evolution in a 30-Year Study of Darwin's Finches. *Science* 296:707-711.
- Hahn, C., M. J. Genner, G. F. Turner, and D. A. Joyce. 2017. The genomic basis of cichlid fish adaptation within the deepwater "twilight zone" of Lake Malawi. *Evolution Letters* 1:184-198.
- Haldane, J. B. S. 1948. The theory of a cline. *Journal of Genetics* 48:277-284.
- Härer, A., A. Meyer, and J. Torres-Dowdall. 2018. Convergent phenotypic evolution of the visual system via different molecular routes: How Neotropical cichlid fishes adapt to novel light environments. *Evolution Letters* 2:341-354.
- Härer, A., J. Torres-Dowdall, and A. Meyer. 2017. Rapid adaptation to a novel light environment: The importance of ontogeny and phenotypic plasticity in shaping the visual system of Nicaraguan Midas cichlid fish (*Amphilophus citrinellus* spp.). *Molecular Ecology* 26:5582-5593.
- Hendry, A. P., and M. T. Kinnison. 1999. Perspective: The Pace of Modern Life: Measuring Rates of Contemporary Microevolution. *Evolution* 53:1637-1653.
- Hereford, J., and A. A. Winn. 2008. Limits to local adaptation in six populations of the annual plant *Diodia teres*. *New Phytologist* 178:888-896.
- Hoekstra, H. E., K. E. Drumm, and M. W. Nachman. 2004. Ecological genetics of adaptive color polymorphism in pocket mice: geographic variation in selected and neutral genes. *Evolution* 58:1329-1341.

- Hofmann, C. M., K. E. O'Quin, N. J. Marshall, T. W. Cronin, O. Seehausen, and K. L. Carleton. 2009. The Eyes Have It: Regulatory and Structural Changes Both Underlie Cichlid Visual Pigment Diversity. *PLoS Biology* 7:e1000266.
- Huey, R. B., G. W. Gilchrist, M. L. Carlson, D. Berrigan, and L. Serra. 2000. Rapid evolution of a geographic cline in size in an introduced fly. *Science* 287:308-309.
- Huxley, J. 1938. Clines: an Auxiliary Taxonomic Principle. *Nature* 142:219-220.
- Irisarri, I., P. Singh, S. Koblmüller, J. Torres-Dowdall, F. Henning, P. Franchini, C. Fischer et al. 2018. Phylogenomics uncovers early hybridization and adaptive loci shaping the radiation of Lake Tanganyika cichlid fishes. *Nature Communications* 9.
- Johnsen, S. 2012, *The Optics of Life: A Biologist's Guide to Light in Nature*, Princeton University Press.
- Karagic, N., A. Harer, A. Meyer, and J. Torres-Dowdall. 2018. Heterochronic opsin expression due to early light deprivation results in drastically shifted visual sensitivity in a cichlid fish: Possible role of thyroid hormone signaling. *J Exp Zool B Mol Dev Evol* 330:202-214.
- Kautt, A. F., C. F. Kratochwil, A. Nater, G. Machado-Schiaffino, M. Olave, F. Henning, J. Torres-Dowdall et al. 2020. Contrasting signatures of genomic divergence during sympatric speciation. *Nature* 588:106-111.
- Kautt, A. F., G. Machado-Schiaffino, and A. Meyer. 2016. Multispecies Outcomes of Sympatric Speciation after Admixture with the Source Population in Two Radiations of Nicaraguan Crater Lake Cichlids. *Plos Genetics* 12:e1006157.
- . 2018. Lessons from a natural experiment: Allopatric morphological divergence and sympatric diversification in the Midas cichlid species complex are largely influenced by ecology in a deterministic way. *Evolution Letters* 2:323-340.
- Kawecki, T. J., and D. Ebert. 2004. Conceptual issues in local adaptation. *Ecology Letters* 7:1225-1241.

- Kirk, J. T. O. 2010, *Light and Photosynthesis in Aquatic Ecosystems*. Cambridge, Cambridge University Press.
- Loew, E. R. 1995. Determinants of visual pigment spectral location and photoreceptor cell spectral sensitivity, Pages 57-77 in M. B. A. Djamgoz, S. N. Archer, and S. Vallerger, eds. *Neurobiology and Clinical Aspects of the Outer Retina*. Dordrecht, Springer Netherlands.
- Loew, E. R., and W. N. McFarland. 1990. The underwater visual environment, Pages 1-43, Springer Netherlands.
- Losos, J. B. 2018, *Improbable destinies: Fate, chance, and the future of evolution*, Penguin.
- Lythgoe, J. N. 1979, *The ecology of vision*. Oxford; New York, Clarendon Press ; Oxford University Press.
- Maccoll, A. D. C. 2011. The ecological causes of evolution. *Trends in Ecology & Evolution* 26:514-522.
- Marques, D. A., J. S. Taylor, F. C. Jones, F. Di Palma, D. M. Kingsley, and T. E. Reimchen. 2017. Convergent evolution of SWS2 opsin facilitates adaptive radiation of threespine stickleback into different light environments. *PLOS Biology* 15:e2001627.
- McFarland, W. N., and F. W. Munz. 1975a. Part II: The photic environment of clear tropical seas during the day. *Vision Research* 15:1063-1070.
- . 1975b. Part III: The evolution of photopic visual pigments in fishes. *Vision Research* 15:1071-1080.
- McNeilly, T. 1968. Evolution in closely adjacent plant populations III. *Agrostis tenuis* on a small copper mine. *Heredity* 23:99-108.
- Mobley, C. 1994, *Light and Water: Radiative Transfer in Natural Waters*.
- Mullen, L. M., and H. E. Hoekstra. 2008. Natural Selection Along An Environmental Gradient: A Classic Cline In Mouse Pigmentation. *Evolution* 62:1555-1570.

- Musilova, Z., F. Cortesi, M. Matschiner, W. I. L. Davies, J. S. Patel, S. M. Stieb, F. De Busserolles et al. 2019. Vision using multiple distinct rod opsins in deep-sea fishes. *Science* 364:588-592.
- Musilova, Z., W. Salzburger, and F. Cortesi. 2021. The Visual Opsin Gene Repertoires of Teleost Fishes: Evolution, Ecology, and Function. *Annual Review of Cell and Developmental Biology* 37:441-468.
- Nosil, P., R. Villoutreix, C. F. De Carvalho, T. E. Farkas, V. Soria-Carrasco, J. L. Feder, B. J. Crespi et al. 2018. Natural selection and the predictability of evolution in *Timema* stick insects. *Science* 359:765-770.
- Novales Flamarique, I. 2016. Diminished foraging performance of a mutant zebrafish with reduced population of ultraviolet cones. *Proc Biol Sci* 283:20160058.
- O'Quin, K. E., C. M. Hofmann, H. A. Hofmann, and K. L. Carleton. 2010. Parallel evolution of opsin gene expression in African cichlid fishes. *Molecular Biology and Evolution* 27:2839-2854.
- Oldfield, R., J. McCrary, and K. McKaye. 2006. Habitat Use, Social Behavior, and Female and Male Size Distributions of Juvenile Midas Cichlids, *Amphilophus cf. citrinellus*, in Lake Apoyo, Nicaragua. *Carib. J. Sci.* 42.
- Partridge, J. C., and M. E. Cummings. 1999. Adaptation of visual pigments to the aquatic environment, Pages 251-283 in S. N. Archer, M. B. A. Djamgoz, E. R. Loew, J. C. Partridge, and S. Vallergera, eds. *Adaptive Mechanisms in the Ecology of Vision*. Dordrecht, Springer Netherlands.
- Pigliucci, M. 2001, *Phenotypic Plasticity: Beyond Nature and Nurture*, Johns Hopkins University Press.
- R Core Team. 2020. *R: A Language and Environment for Statistical Computing*. R Foundation for Statistical Computing, Vienna, Austria.

- Reimchen, T. E., and C. A. Bergstrom. 2023. Multi-generation selective landscapes and sub-lethal injuries in stickleback. *Evolution* 77:1101-1116.
- Rennison, D. J., G. L. Owens, N. Heckman, D. Schluter, and T. Veen. 2016. Rapid adaptive evolution of colour vision in the threespine stickleback radiation. *Proc Biol Sci* 283.
- Reznick, D., and J. A. Endler. 1982. The impact of predation on life history evolution in Trinidadian guppies (*Poecilia reticulata*). *Evolution*:160-177.
- Riesch, R., M. Plath, and D. Bierbach. 2018. Ecology and evolution along environmental gradients. *Current Zoology* 64:193-196.
- Rio, D. C., M. Ares, G. J. Hannon, and T. W. Nilsen. 2010. Purification of RNA using TRIzol (TRI reagent). *Cold Spring Harbor Protocols* 2010:pdb. prot5439.
- Sabbah, S., S. M. Gray, E. S. Boss, J. M. Fraser, R. Zatha, and C. W. Hawryshyn. 2011. The underwater photic environment of Cape Maclear, Lake Malawi: comparison between rock- and sand-bottom habitats and implications for cichlid fish vision. *Journal of Experimental Biology* 214:487-500.
- Sabbah, S., R. L. Laria, S. M. Gray, and C. W. Hawryshyn. 2010. Functional diversity in the color vision of cichlid fishes. *BMC Biology* 8:133.
- Sakai, Y., S. Kawamura, and M. Kawata. 2018. Genetic and plastic variation in opsin gene expression, light sensitivity, and female response to visual signals in the guppy. *Proceedings of the National Academy of Sciences of the USA* 115:12247-12252.
- Sand, H., G. Cederlund, and K. Danell. 1995. Geographical and latitudinal variation in growth patterns and adult body size of Swedish moose (*Alces alces*). *Oecologia* 102:433-442.
- Schluter, D. 2000, *The ecology of adaptive radiation*, OUP Oxford.
- Schneider, R. F., S. J. Rometsch, J. Torres-Dowdall, and A. Meyer. 2020. Habitat light sets the boundaries for the rapid evolution of cichlid fish vision, while sexual selection can tune it within those limits. *Molecular Ecology* 29:1476-1493.

- Schott, R. K., S. P. Refvik, F. E. Hauser, H. López-Fernández, and B. S. W. Chang. 2014. Divergent Positive Selection in Rhodopsin from Lake and Riverine Cichlid Fishes. *Molecular Biology and Evolution* 31:1149-1165.
- Schweikert, L. E., R. R. Fitak, E. M. Caves, T. T. Sutton, and S. Johnsen. 2018. Spectral sensitivity in ray-finned fishes: diversity, ecology and shared descent. *Journal of Experimental Biology* 221.
- Seehausen, O., J. J. M. v. Alphen, and F. Witte. 1997. Cichlid Fish Diversity Threatened by Eutrophication That Curbs Sexual Selection. *Science* 277:1808-1811.
- Seehausen, O., Y. Terai, I. S. Magalhaes, K. L. Carleton, H. D. Mrosso, R. Miyagi, I. van der Sluijs et al. 2008. Speciation through sensory drive in cichlid fish. *Nature* 455:620-626.
- Smith, A. R., K. Ma, D. Soares, and K. L. Carleton. 2012. Relative LWS cone opsin expression determines optomotor thresholds in Malawi cichlid fish. *Genes Brain Behav* 11:185-192.
- Solomon, C. T., S. E. Jones, B. C. Weidel, I. Buffam, M. L. Fork, J. Karlsson, S. Larsen et al. 2015. Ecosystem Consequences of Changing Inputs of Terrestrial Dissolved Organic Matter to Lakes: Current Knowledge and Future Challenges. *Ecosystems* 18:376-389.
- Sotka, E. E. 2008. *Clines*, Pages 613-618, Elsevier.
- Spady, T. C., O. Seehausen, E. R. Loew, R. C. Jordan, T. D. Kocher, and K. L. Carleton. 2005. Adaptive Molecular Evolution in the Opsin Genes of Rapidly Speciating Cichlid Species. *Molecular Biology and Evolution* 22:1412-1422.
- Stoffel, M. A., S. Nakagawa, and H. Schielzeth. 2021. partR2: partitioning R2 in generalized linear mixed models. *PeerJ* 9:e11414.
- Stomp, M., J. Huisman, L. J. Stal, and H. C. P. Matthijs. 2007. Colorful niches of phototrophic microorganisms shaped by vibrations of the water molecule. *The ISME Journal* 1:271-282.
- Sugawara, T., Y. Terai, H. Imai, G. F. Turner, S. Koblmuller, C. Sturmbauer, Y. Shichida et al. 2005. Parallelism of amino acid changes at the RH1 affecting spectral sensitivity among



- deep-water cichlids from Lakes Tanganyika and Malawi. *Proc. Natl. Acad. Sci. USA* 102:5448-5453.
- Svensson, E. I. 2023. Phenotypic selection in natural populations: what have we learned in 40 years? *Evolution* 77:1493-1504.
- Tobler, M., J. L. Kelley, M. Plath, and R. Riesch. 2018. Extreme environments and the origins of biodiversity: Adaptation and speciation in sulphide spring fishes. *Molecular Ecology* 27:843-859.
- Torres-Dowdall, J., F. Henning, K. R. Elmer, and A. Meyer. 2015. Ecological and Lineage-Specific Factors Drive the Molecular Evolution of Rhodopsin in Cichlid Fishes. *Molecular Biology and Evolution* 32:2876-2882.
- Torres-Dowdall, J., G. Machado-Schiaffino, A. F. Kautt, H. Kusche, and A. Meyer. 2014. Differential predation on the two colour morphs of Nicaraguan Crater lake Midas cichlid fish: implications for the maintenance of its gold-dark polymorphism. *Biological Journal of the Linnean Society* 112:123-131.
- Torres-Dowdall, J., and A. Meyer. 2021. Sympatric and Allopatric Diversification in the Adaptive Radiations of Midas Cichlids in Nicaraguan Lakes, Pages 175-216 *in* M. E. Abate, and D. L. G. Noakes, eds. *The Behavior, Ecology and Evolution of Cichlid Fishes*. Dordrecht, Springer Netherlands.
- Torres-Dowdall, J., M. E. R. Pierotti, A. Harer, N. Karagic, J. M. Woltering, F. Henning, K. R. Elmer et al. 2017. Rapid and Parallel Adaptive Evolution of the Visual System of Neotropical Midas Cichlid Fishes. *Molecular Biology and Evolution* 34:2469-2485.
- Torres-Dowdall, J., N. Karagic, A. Härer, and A. Meyer. 2021. Diversity in visual sensitivity across Neotropical cichlid fishes via differential expression and intraretinal variation of opsin genes. *Molecular Ecology* 30:1880-1891.
- Veen, T., C. Brock, D. Rennison, and D. Bolnick. 2017. Plasticity contributes to a fine-scale depth gradient in sticklebacks' visual system. *Molecular Ecology* 26:4339-4350.

- Wald, G. 1939. The Porphyropsin Visual System. *Journal of General Physiology* 22:775-794.
- Williams, G. C. 1966. *Adaptation and Natural Selection*, Princeton university press.
- Wright, S. 1932. The roles of mutation, inbreeding, crossbreeding, and selection in evolution. *Proceedings of the Sixth International Congress of Genetics* 8:356-366.
- Yokoyama, S. 2000. Molecular evolution of vertebrate visual pigments. *Progress in Retinal and Eye Research* 19:385-419.
- . 2008. Evolution of dim-light and color vision pigments. *Annual Review of Genomics and Human Genetics* 9:259-282.
- Yourick, M. R., B. A. Sandkam, W. J. Gammerdinger, D. Escobar-Camacho, S. P. Nandamuri, F. E. Clark, B. Joyce et al. 2019. Diurnal variation in opsin expression and common housekeeping genes necessitates comprehensive normalization methods for quantitative real-time PCR analyses. *Molecular Ecology Resources* 19:1447-1460.

### **References Cited Only in the Online Enhancements**

- Gingerich, P. D. 1993. Quantification and comparison of evolutionary rates. *American Journal of Science* 293:453.

## Figure Legends

**Figure 1:** A, Breeding pairs of dark (left) and gold (right) color morphs of *Amphilophus sagittae* (Photos from Ad Konings) B, Map showing the Nicaraguan great lakes, crater lakes and one riverine population. Inserts depict the photic environment at 1m depth with spectral curves showing the normalized downwelling irradiance ( $E_d$ ). Vertical solid lines below each spectral curve represent the spectrum-halving wavelength ( $\lambda P_{50}$ ) within the colored area depicting the spectral bandwidth and its color intensity representing the relative luminosity ( $\%E_d$ ). The shaded area in the background of the crater lake inserts shows the photic environment plus  $\lambda P_{50}$  (dashed line) of the respective source great lake.

**Figure 2:** Proportional opsin gene expression from wild-caught fish showing groups of derived crater lake (blue) and its respective source great lake (red) within each panel. River San Juan shown in orange. Bars represent the mean value for each population. Upper right corner shows F-values and significance from ANOVA (type II) using location as the predictor variable. Letters display groups based on Tukey's HSD. Great Lake Managua is considered the predominant source population for the admixed Crater Lake Masaya based on Kautt et. al 2018; 2020.

**Figure 3:** Correlation of shift in spectral sensitivity curves ( $\Delta SSC$ , Fig. S5) and localized spectral attenuation coefficients ( $\Delta K_d$ , Fig. S4) between derived populations and their source population, either Great Lake Nicaragua (Crater Lake Apoyo, depicted with an asterisk) or Great Lake Managua. Great Lake Managua is considered the predominant source population for the admixed Crater Lake Masaya based on Kautt et. al 2018; 2020.

**Figure 4:** A, Individual sensitivity index (PSI) is predicted by the photic environment at the lake of origin (z-scores of PC1 from photic parameters, Table S4). Mean regression lines and 95% confidence intervals (CI) for wild-caught (solid line) and lab-reared (dashed line) individuals. Lower-right corner shows F-values (ANOVA III) for predictor variables; photic environment, rearing environment, and their interaction. B, Mean regression line and 95% CI of coefficients of variation in PSI within each population for wild-caught fish in response to ambient photic environment (PC1). Lower-left corner shows F-value (ANOVA II).  $p < 0.001 = \text{'****'}$ ,  $p < 0.01 = \text{'***'}$ ,  $p > 0.05 = \text{NS}$ .

Figure 1

This is the author's accepted manuscript without copyediting, formatting, or final corrections. It will be published in its final form in an upcoming issue of The American Naturalist, published by The University of Chicago Press. Include the DOI when citing or quoting: <https://doi.org/10.1086/729420>. Copyright 2024 The University of Chicago.

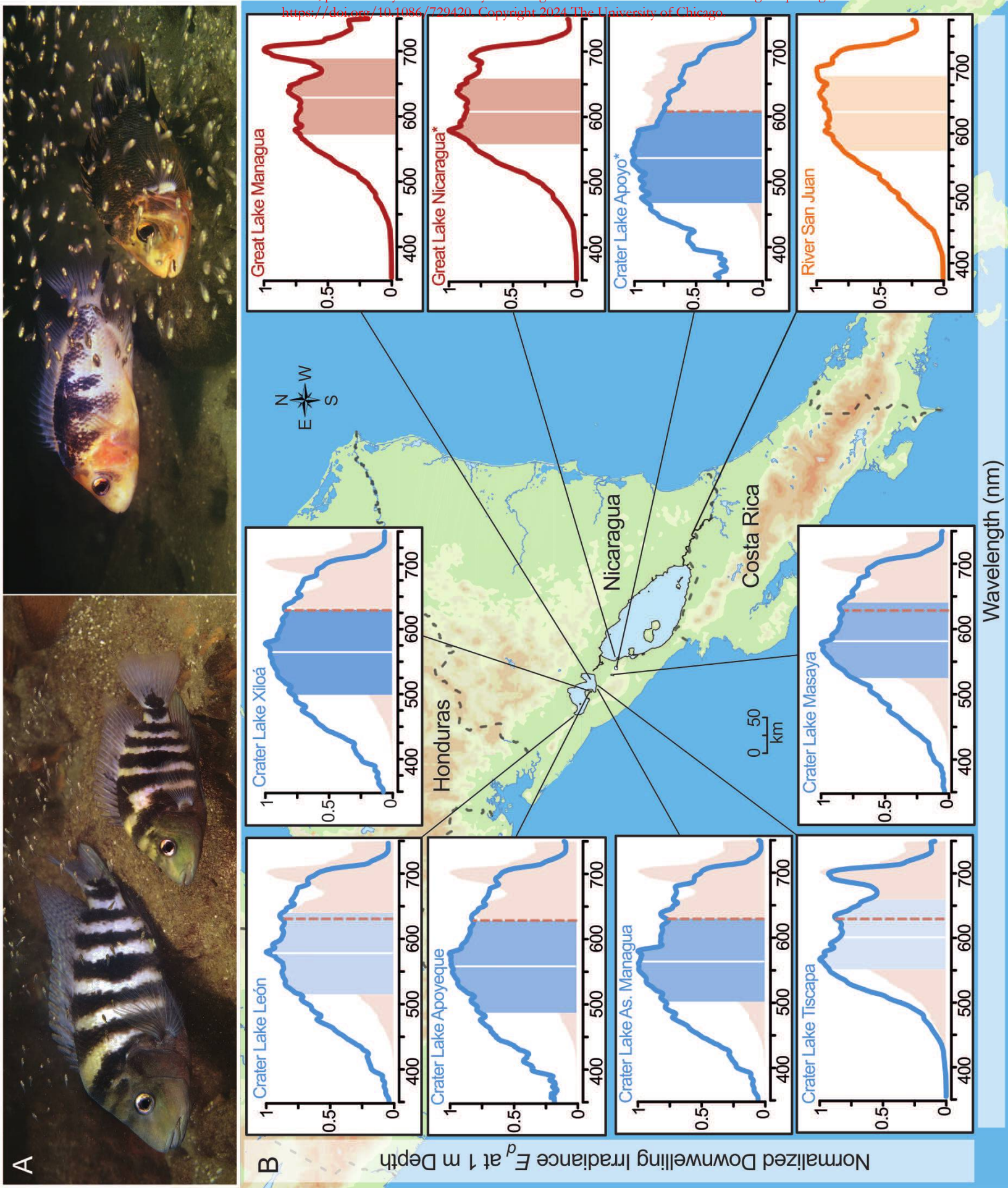


Figure 2

This is the author's accepted manuscript. It will be published in its final form in an upcoming issue of The American Naturalist, published by The University of Chicago Press. Include the DOI when citing or quoting: <https://doi.org/10.1086/729420>. Copyright 2024 The University of Chicago.

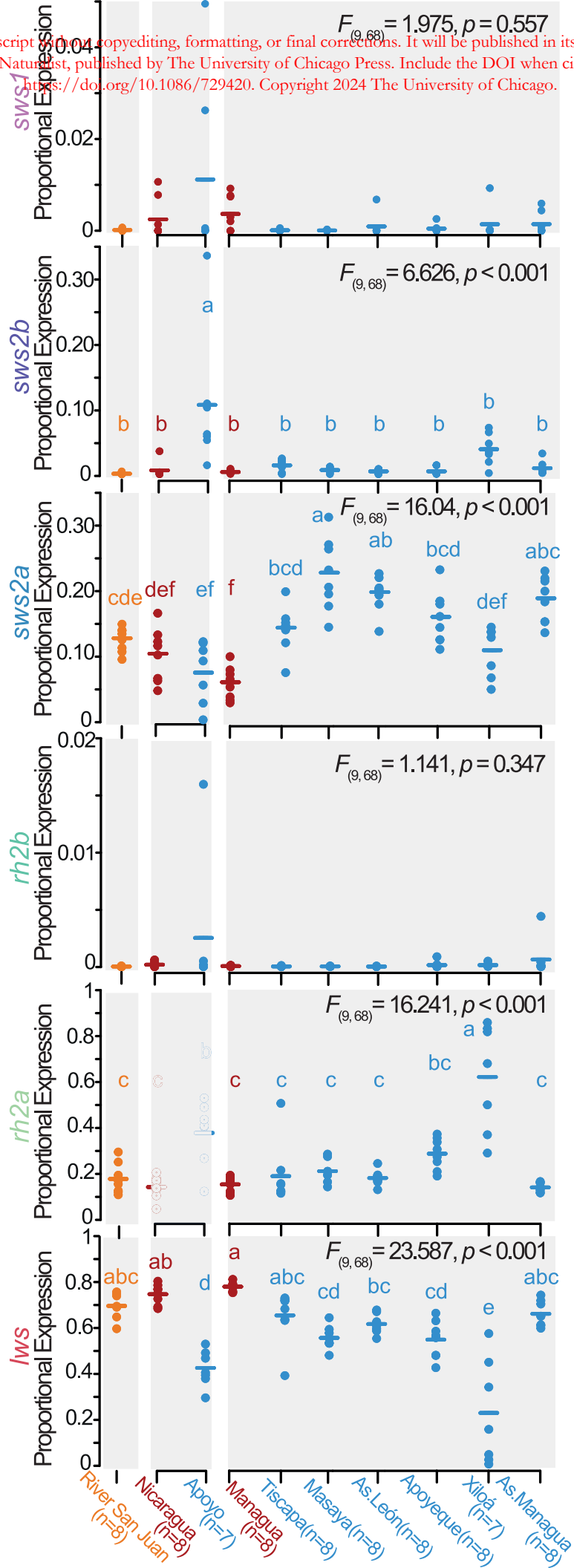


Figure 3

This is the author's accepted manuscript without copyediting, formatting, or final corrections. It will be published in its final form in an upcoming issue of The American Naturalist, published by The University of Chicago Press. Include the DOI when citing or quoting: <https://doi.org/10.1086/729420>. Copyright 2024 The University of Chicago.

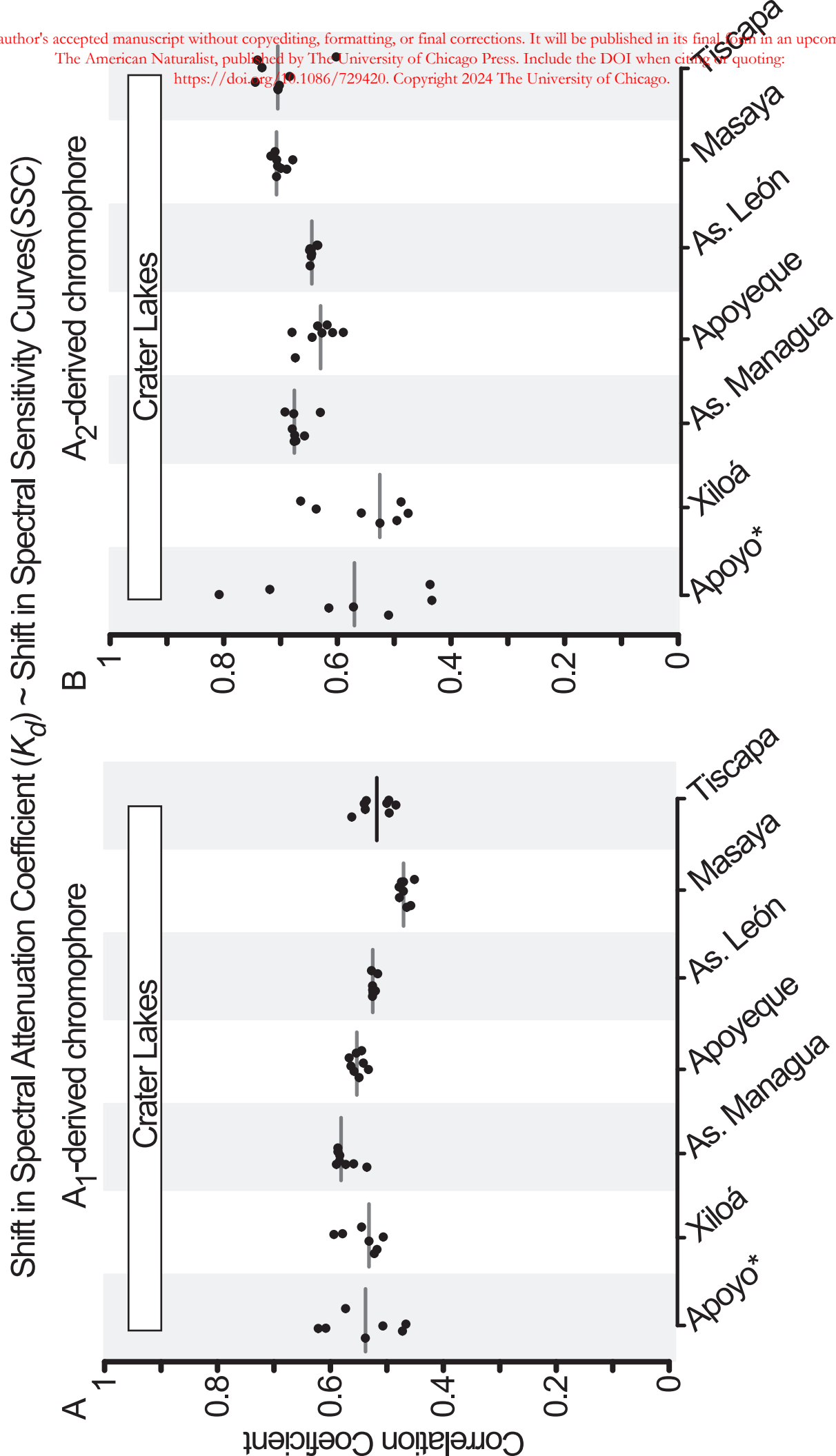
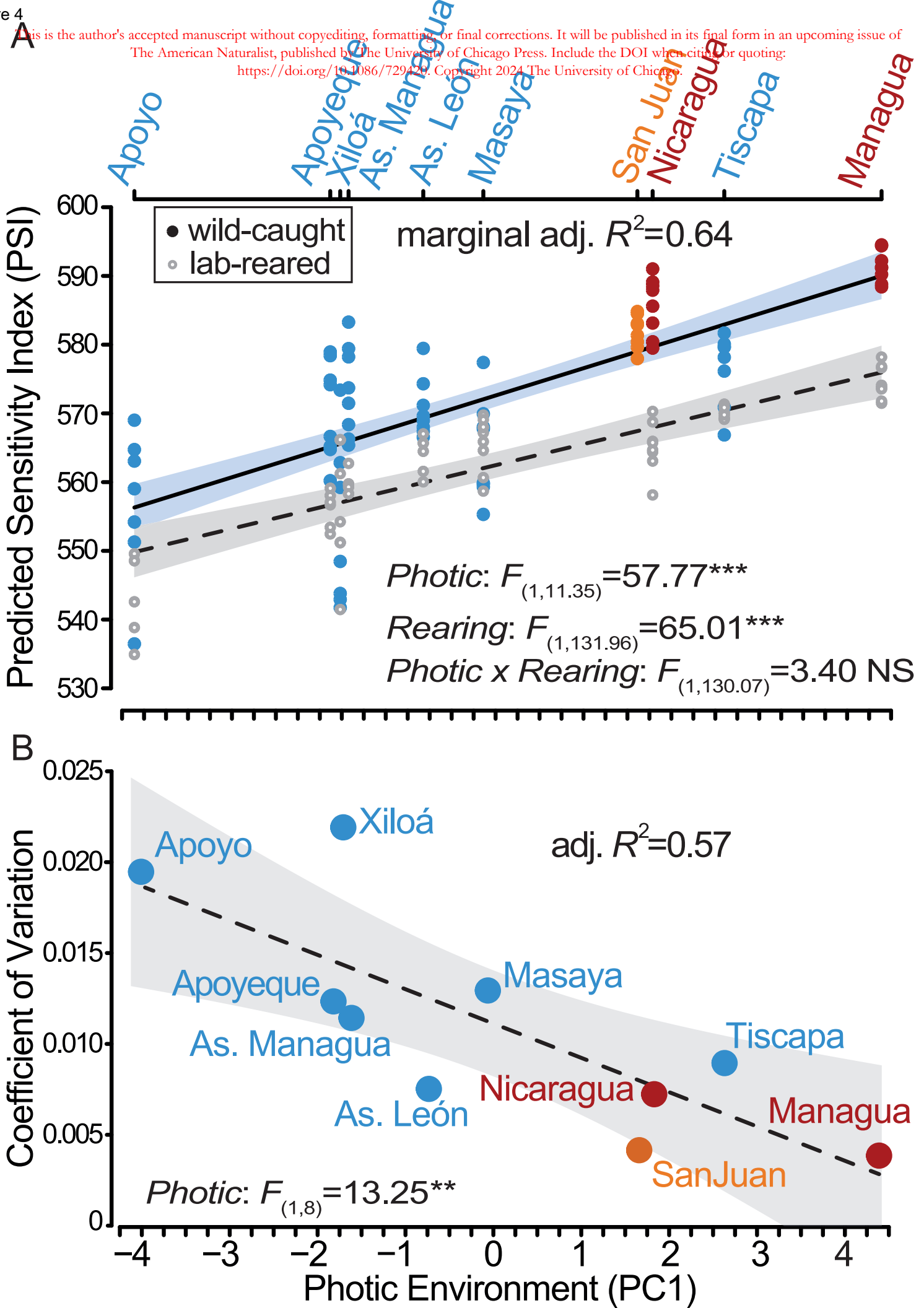


Figure 4



## Supplemental Information for:

### Repeated Divergence in Opsin Genes Expression Mirrors Photic Habitat Changes in Rapidly Evolving Crater Lake Cichlid Fishes

César Bertinetti<sup>1,2</sup>, Andreas Härer<sup>1,3</sup>, Nidal Karagic<sup>1,4</sup>, Axel Meyer<sup>1</sup>, Julián Torres-Dowdall<sup>1,2</sup>

Published in *The American Naturalist*

<sup>1</sup> Zoology and Evolutionary Biology, Department of Biology, University of Konstanz, Konstanz, Germany

<sup>2</sup> Department of Biological Sciences, University of Notre Dame, Notre Dame, IN, USA

<sup>3</sup> current address: School of Biological Sciences, Department of Ecology, Behavior, & Evolution, University of California San Diego, La Jolla, CA, USA

<sup>4</sup> current address: Biotechnological Institute, University of Helsinki, Helsinki, Finland

Corresponding author: Julián Torres-Dowdall, Email: [torresdowdall@nd.edu](mailto:torresdowdall@nd.edu)

## Table of Contents

<b>Table S1</b> Individuals of Midas cichlids species complex from each location included in this study. ....	3
<b>Table S2.</b> List of primer sequences used for RT-qPCR in this study based on Torres-Dowdall et al. (2017).....	4
<b>Table S3.</b> Amplification efficiencies for opsin gene primers used in this study. ....	4
<b>Table S4.</b> Output of correlation based Principal Components Analysis (PCA) of scaled photic variables across all habitats.....	5
<b>Table S5.</b> Evolutionary rates of spectral sensitivity in Midas cichlids across the Nicaraguan crater lakes. Demographic history and generation time of 1.5 years based on Kautt et al. (2020); Kautt et al. (2018). Haldanes calculated based on Gingerich (1993). ....	5
<b>Table S6.</b> Robustness value from sensitivity analysis accounting for unobserved confounding factors based on Cinelli and Hazlett (2020). ....	6
<b>Figure S1.</b> Logarithmic median absolute irradiance for all sites and depths for downwelling, sidewelling and upwelling measurements.....	8



**Figure S2.** Map of Nicaragua, showing the location of the great and crater lakes. Inserts within the map depict the photic environment of the different lakes. Solid lines show the normalized sidewelling irradiance ( $E_s$ ) at one meter depth for each lake. The shaded area displayed in the background of the crater lake inserts shows the photic environment of the respective source great lake based on Midas cichlids colonization history Kautt et al. (2016; 2020). ..... 9

**Figure S3.** Summarized visualization of the geometric mean of expression in reference genes (*imp2*, *gapdh*) measured via qPCR for (a) wild-caught and (b) lab-reared individuals. .... 10

**Figure S4.** Localized spectral coefficient of downwelling irradiance across the Nicaraguan lakes ( $K_d$ ) calculated according to Sabbah et al. (2011). Dashed lines depict respective source great lake. Values closer to one represent higher extinction rate where light is poorly transmitted through the water body (Rennison et al. 2016). ..... 11

**Figure S5.** Normalized spectral sensitivity assuming  $A_2$ -chromophore usage based on opsin expression (see Fig. 2) of wild-caught individuals based on templates from Govardovskii et al. (2000) and opsin absorbance peaks from Torres-Dowdall et al. (2017). Individual sensitivities are shown as solid lines for each location while shaded area depicts the mean ( $\pm$  SEM) sensitivity of the respective ancestral great lake..... 12

**Figure S6.** Correlation of shift in spectral sensitivity curves ( $\Delta$ SSC) and normalized spectral irradiance ( $\Delta$ E) between derived populations and their ancestral population, either great lake Nicaragua (crater lake Apoyo, depict with an asterisk) or great lake Managua. Changes in downwelling irradiance ( $\Delta E_d$ , Fig. 1) for  $A_1$ -chromophore (a) and  $A_2$ -chromophore (b). Changes in sidewelling irradiance ( $\Delta E_s$ , Fig. S2) for  $A_1$ -chromophore (c) and  $A_2$ -chromophore (d). Bars show the median for the correlation coefficients for each population. Black dots ( $p > 0.05$ ) after adjusting for multiple testing using Benjamini-Hochberg FDR..... 13

**Figure S7.** Biplot depicting the PCA scores generated from variables of photic conditions of all habitat at one meter depth (Table S4). Arrows represent the loadings of each variable. 14

**Figure S8.** Proportional opsin gene expression from lab-reared individuals. Bars represent mean value for each population. F-values and significance from ANOVA analysis using location as predictor variable is shown on upper-right. Letters display groups based on Tukey's HSD. Great lakes are shown in red, while crater lakes are in blue. .... 15

**Figure S9.** Proportion of variance in spectral sensitivity explained by photic environment, rearing conditions and its interaction (fixed effects). Dots represent mean  $R^2$  with 95% confidence intervals estimated via bootstrapping (iterations=1000) as described in Stoffel et al. (2021). ..... 16

**Figure S10.** Diagnostic plot for linear mixed-effect model shown in Fig. S6 ..... 16

**Table S1** Individuals of Midas cichlids species complex from each location included in this study.

Location	Species	N° of fish (wild-caught)	N° of fish (lab-reared)
Crater Lake Apoyo	<i>Amphilophus astorquii</i>	7	5 (4) <sup>a</sup>
Crater Lake As. Managua	<i>Amphilophus tolteca</i>	8	6
Crater Lake Xiloá	<i>Amphilophus sagittae</i> & <i>Amphilophus xiloaensis</i>	7	8 (8) <sup>a</sup>
Crater Lake Apoyeque	<i>Amphilophus</i> cf. <i>citrinellus</i>	8	6
Crater Lake As. León	<i>Amphilophus</i> cf. <i>citrinellus</i>	8	6
Crater Lake Masaya	<i>Amphilophus</i> cf. <i>citrinellus</i>	8	9 (4) <sup>a</sup>
Crater Lake Tiscapa	<i>Amphilophus</i> cf. <i>citrinellus</i>	8	6
Great Lake Nicaragua	<i>Amphilophus</i> cf. <i>citrinellus</i>	8	8 (7) <sup>a</sup>
Great Lake Managua	<i>Amphilophus</i> cf. <i>citrinellus</i>	8	8
River San Juan	<i>Amphilophus</i> cf. <i>citrinellus</i>	8	-

a - Opsin gene expression values from Torres-Dowdall et al. (2017)

**Table S2.** List of primer sequences used for RT-qPCR in this study based on Torres-Dowdall et al. (2017)

GENE	NAME	SEQUENCE
<i>sws1</i>	AH_SWS1_F2	GATATACCTGCTCCAGCCAAAG
<i>sws1</i>	AH_SWS1_R2	GGTCATCTGTAAACCATTTGGAG
<i>sws2b</i>	AH_SWS2B_F1	CACGAACGGAAGCTGCTTATTG
<i>sws2b</i>	AH_SWS2B_R1	GCCATTTGACCTGAGACTGG
<i>sws2a</i>	JTD_SWS2a_F1.1	GAAACTTCGATCCCACCTCA
<i>sws2a</i>	JTD_SWS2a_R4	GGCTTACCATAACCACCGAGT
<i>rh2b</i>	AH_RH2B_F1	GCTTGCAGCAGCCTTCAC
<i>rh2b</i>	AH_RH2B_R1	CCTGTGGACCGGACTACTACAC
<i>rh2a</i>	JTD_RH2Aalpha_F2.1	TGGTGCTGGGGTACTTTTTG
<i>rh2a</i>	JTD_RH2A_R3	CTCATTGTTGAAGCCTGGAG
<i>lws</i>	JTD_LWS_F1.1	GGCGGTACCATGAAGATACAAC
<i>lws</i>	JTD_LWS_R4.1	ACCACGAAAAGCATCCAGAG
<i>imp2</i>	AH_IMP2_F1	GCCTGGAGCATGTTGACC
<i>imp2</i>	AH_IMP2_R1	CGAAGTGACGGATCTTACGG
<i>gapdh2</i>	GAPDH2_F1	TGCCCATACAAACATCATTCC
<i>gapdh2</i>	GAPDH2_R1	GGCATGTCAGATCCACCACT

**Table S3.** Amplification efficiencies for opsin gene primers used in this study.

GENE	EFFICIENCY
<i>sws1</i>	2.027
<i>sws2b</i>	2.031
<i>sws2a</i>	2.010
<i>rh2b</i>	1.986
<i>rh2a</i>	1.999
<i>lws</i>	2.063

**Table S4.** Output of correlation based Principal Components Analysis (PCA) of scaled photic variables across all habitats.

	PC1	PC2	PC3	PC4	PC5	PC6	PC7
Standard deviation	2.5580	0.5833	0.2538	0.1848	0.2010	0.0463	0.0222
Proportion of Variance	0.9350	0.0486	0.0092	0.0057	0.0010	0.0003	0.0001
Cumulative Proportion	0.9302	0.9836	0.9928	0.9985	0.9996	0.9999	1.0000
Loadings:							
Downwelling $\lambda$ P50	0.3884	-0.0808	0.2040	0.3984	0.3702	0.0345	-0.7098
Downwelling $\lambda$ P25	0.3849	0.0066	0.6000	0.3461	-0.5005	0.1634	0.3076
Downwelling $\lambda$ P75	0.3844	-0.1363	-0.5091	0.4759	0.2009	0.3003	0.4661
Relative Luminosity	0.3284	-0.9272	0.0949	0.1306	-0.0751	0.0218	-0.0116
Sidewelling $\lambda$ P50	0.3859	-0.2300	-0.1855	0.2668	0.2123	0.7973	0.1061
Sidewelling $\lambda$ P25	0.3836	-0.1961	-0.0370	0.5794	0.3061	0.4578	0.1953
Sidewelling $\lambda$ P75	0.3861	-0.1529	-0.3981	0.2660	-0.6538	0.1898	-0.3669
Positions:							
Crater Lake Apoyo	4.1099	0.0839	0.0595	0.1029	-0.0487	0.0440	-0.0254
Crater Lake Xiloa	1.7677	-0.4963	-0.0529	0.0202	-0.0621	0.0971	0.0295
Crater Lake Apoyeque	1.8227	0.0003	-0.4139	0.0077	0.1584	0.0455	0.0268
Crater Lake As. Managua	1.6728	0.1219	-0.0368	0.0287	-0.1081	0.0119	-0.0067
Crater Lake As. León	0.8228	0.2966	0.2937	0.2010	0.0001	0.0039	0.0046
Crater Lake Masaya	0.1394	-0.7100	0.0674	0.3323	0.0737	0.0109	-0.0344
Crater Lake Tiscapa	2.6019	1.1103	-0.2500	0.1520	-0.0645	0.0167	-0.0122
Great Lake Nicaragua	1.7871	0.0016	0.2920	0.1993	-0.0797	0.0628	0.0342
Great Lake Managua	4.3917	-0.8694	-0.2176	0.2599	-0.0619	0.0151	-0.0128
River San Juan	1.6133	0.4608	0.2586	0.1190	0.1928	0.0348	-0.0036

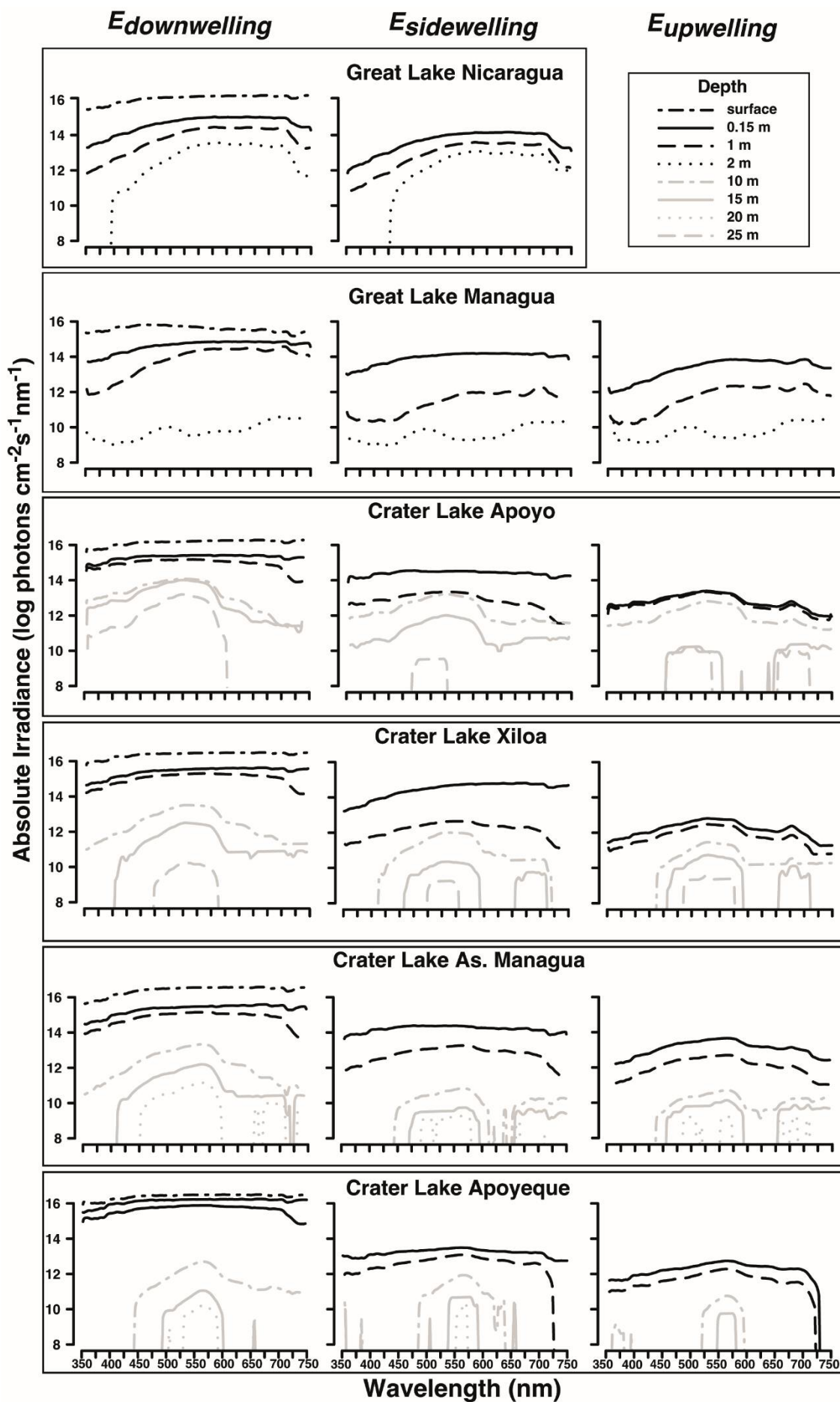
**Table S5.** Evolutionary rates of spectral sensitivity in laboratory-reared Midas cichlids across the Nicaraguan crater lakes. Demographic history and generation time of 1.5 years based on Kautt et al. (2020); Kautt et al. (2018). Haldanes calculated based on Gingerich (1993).

Crater Lake	Number specimens	Mean PSI_A2	Standard Deviation PSI_A2	Number of Generations	Haldanes
Apoyeque	6	556.229	2.625	600.0	0.01218
Apoyo	5	543.002	6.252	3133.3	0.00148
As. León	6	564.162	2.699	1200.0	0.00342
As. Managua	6	559.760	1.629	800.0	0.00869
Masaya	9	565.840	3.806	1866.7	0.00145
Tiscapa	6	570.181	0.861	533.3	0.00428
Xiloá	8	557.320	9.132	2866.7	0.00090

**Table S6.** Robustness value from sensitivity analysis accounting for unobserved confounding factors on outcome PSI\_A2 based on Cinelli and Hazlett (2020).

Treatment	Coefficient of Estimate	Standard Error	t-value	$R^2_{Y \sim D X}$ (%)	$RV_{q=1}$ (%)	$RV_{q=1, \alpha=0.05}$ (%)
Photic	4.031	10.35	11.529	49.4	61.4	54.9

Note.- df = 136; Bound (1x Rearing):  $R^2_{Y \sim Z|X,D} = 46.8\%$ ,  $R^2_{D \sim Z|X} = 0\%$ .



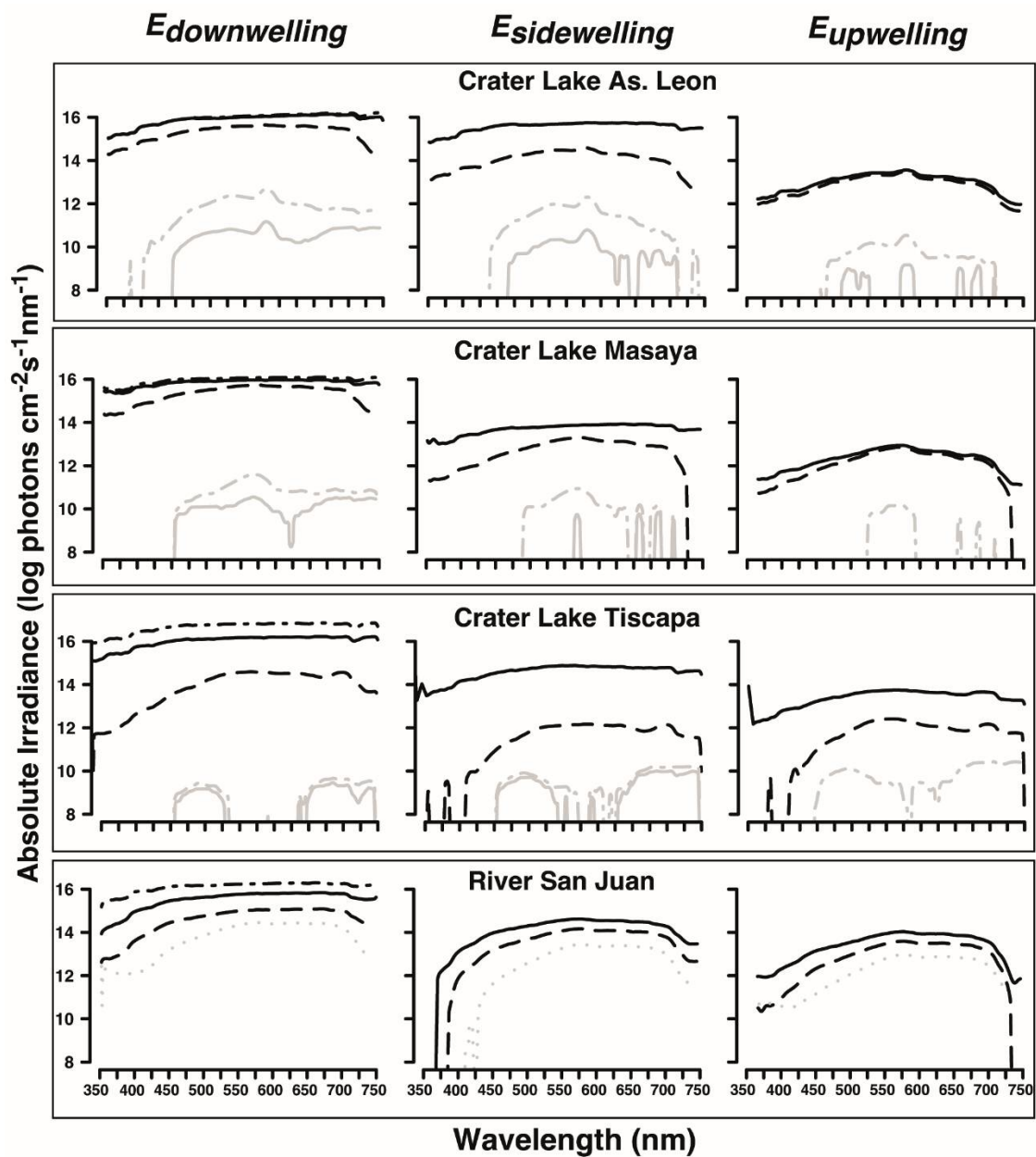


**Figure S1.** Logarithmic median absolute irradiance for all sites and depths for downwelling, sidewelling and upwelling measurements.

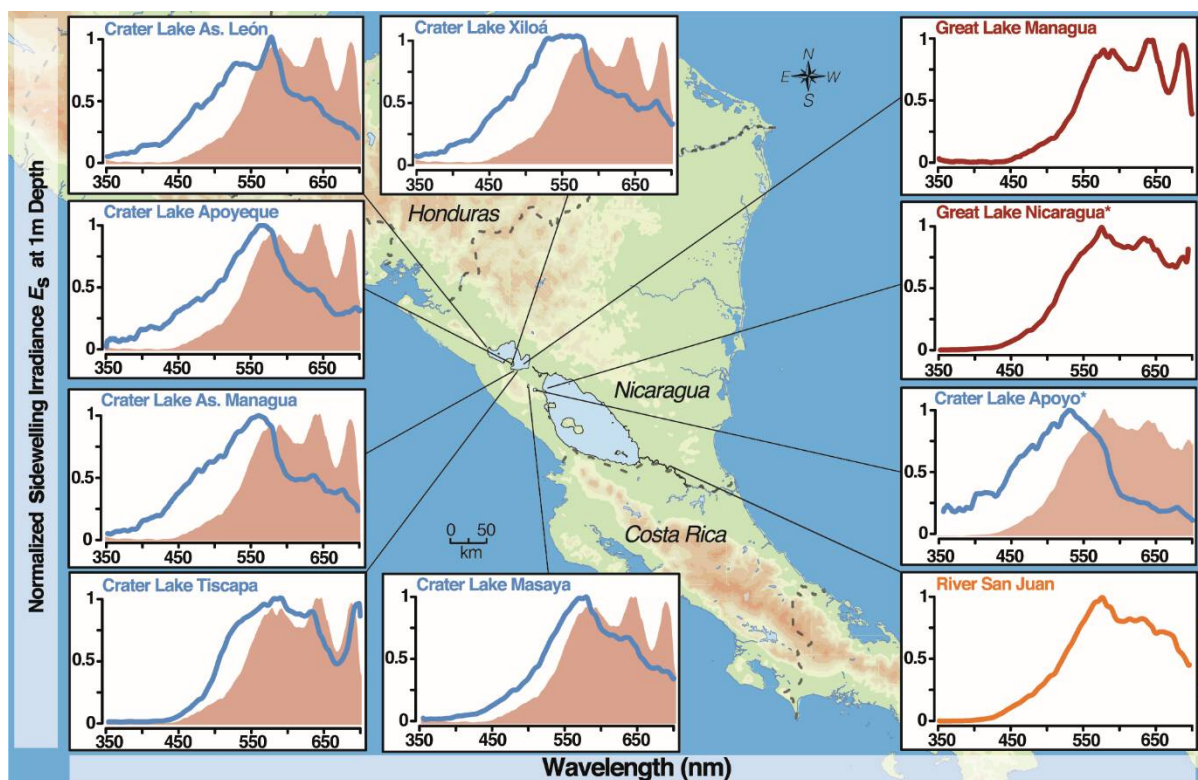


**Figure S2.** Map of Nicaragua, showing the location of the great and crater lakes. Inserts within the map depict the photic environment of the different lakes. Solid lines show the normalized sidewelling irradiance ( $E_s$ ) at one meter depth for each lake. The shaded area displayed in the background of the crater lake inserts shows the photic environment of the respective source great lake based on Midas cichlids colonization history Kautt et al. (2016; 2020). Great Lake Managua is considered the predominant source population for the admixed Crater Lake Masaya based on Kautt et. al 2020.



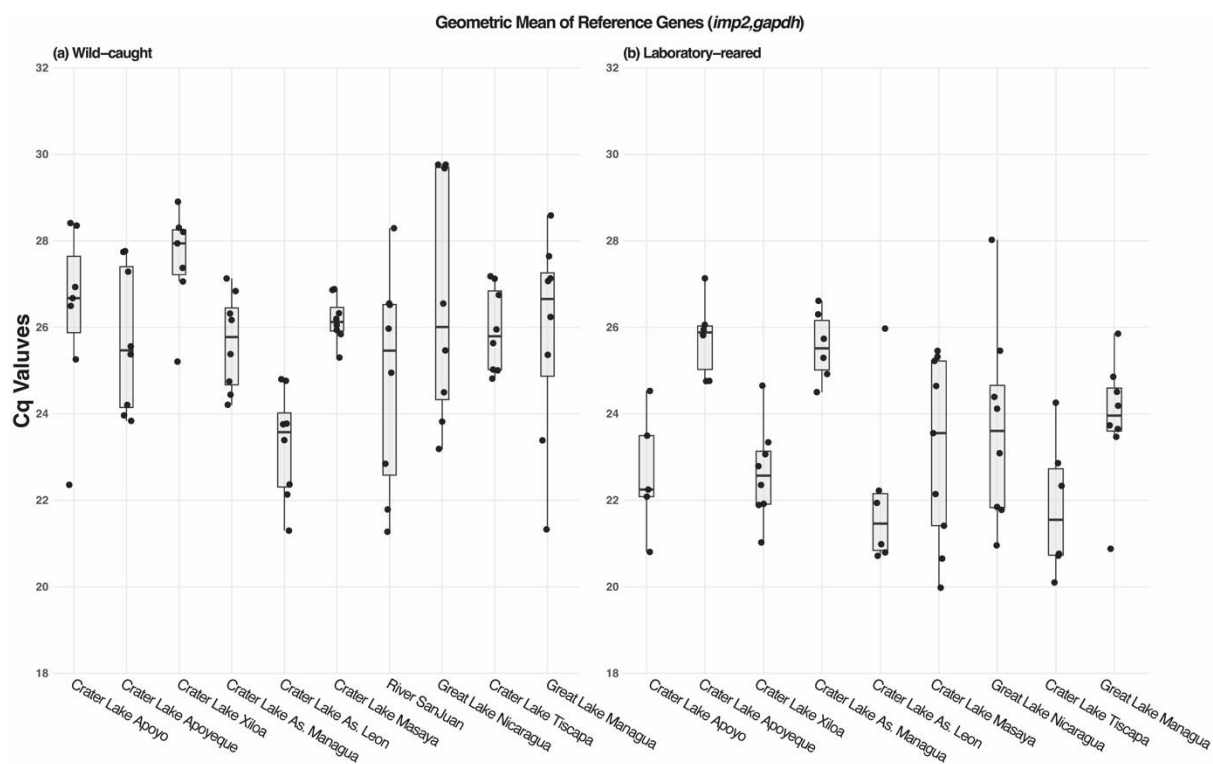


**Figure S3.** Summarized visualization of the geometric mean of expression in reference genes (*imp2, gapdh*) measured via qPCR for (a) wild-caught and (b) lab-reared individuals.

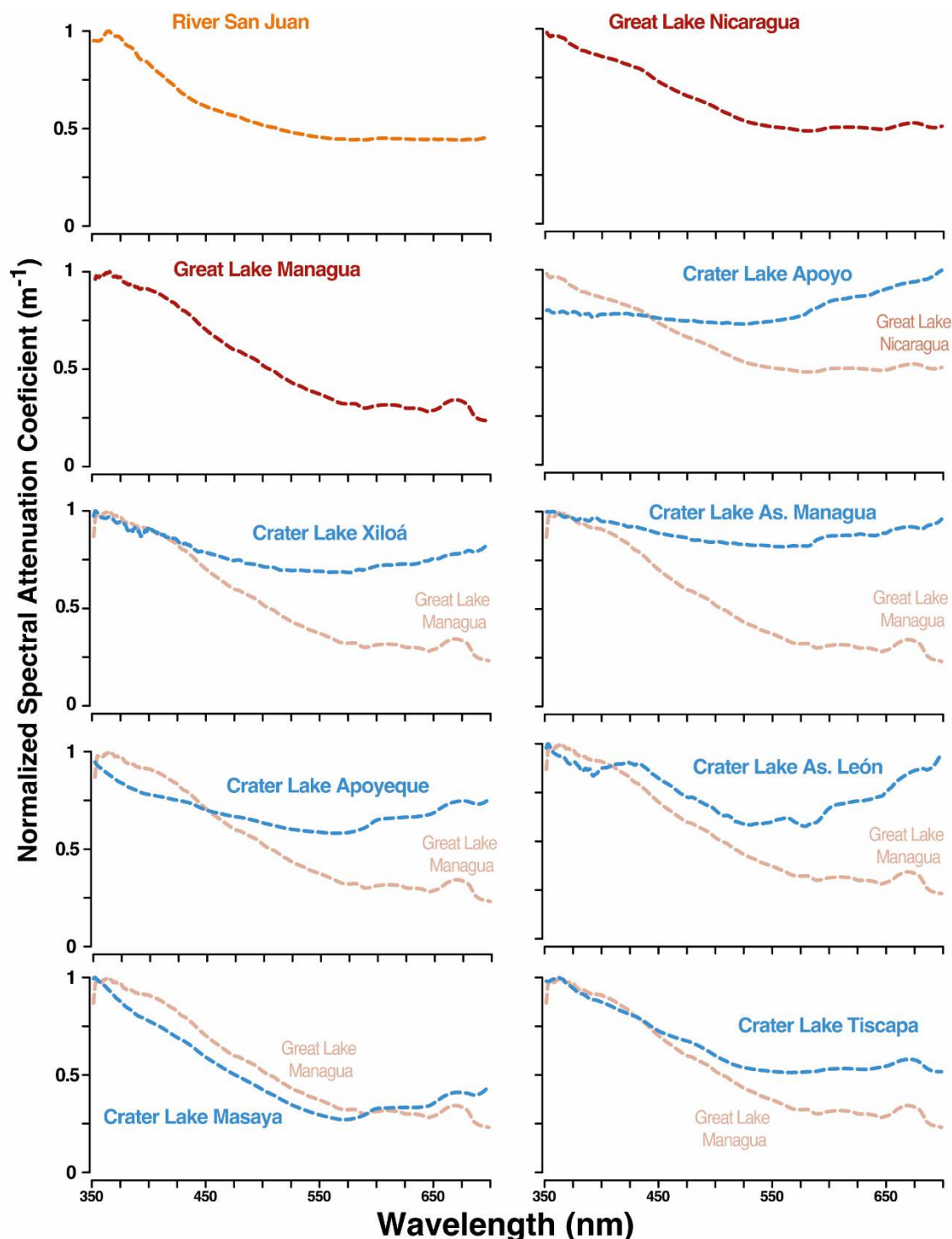


**Figure S4.** Localized spectral coefficient of downwelling irradiance across the Nicaraguan lakes ( $K_d$ ) calculated according to Sabbah et al. (2011). Dashed lines depict respective source great lake. Values closer to one represent higher extinction rate where light is poorly transmitted through the water body (Rennison et al. 2016). Great Lake Managua is considered the predominant source population for the admixed Crater Lake Masaya based on Kautt et. al 2020.

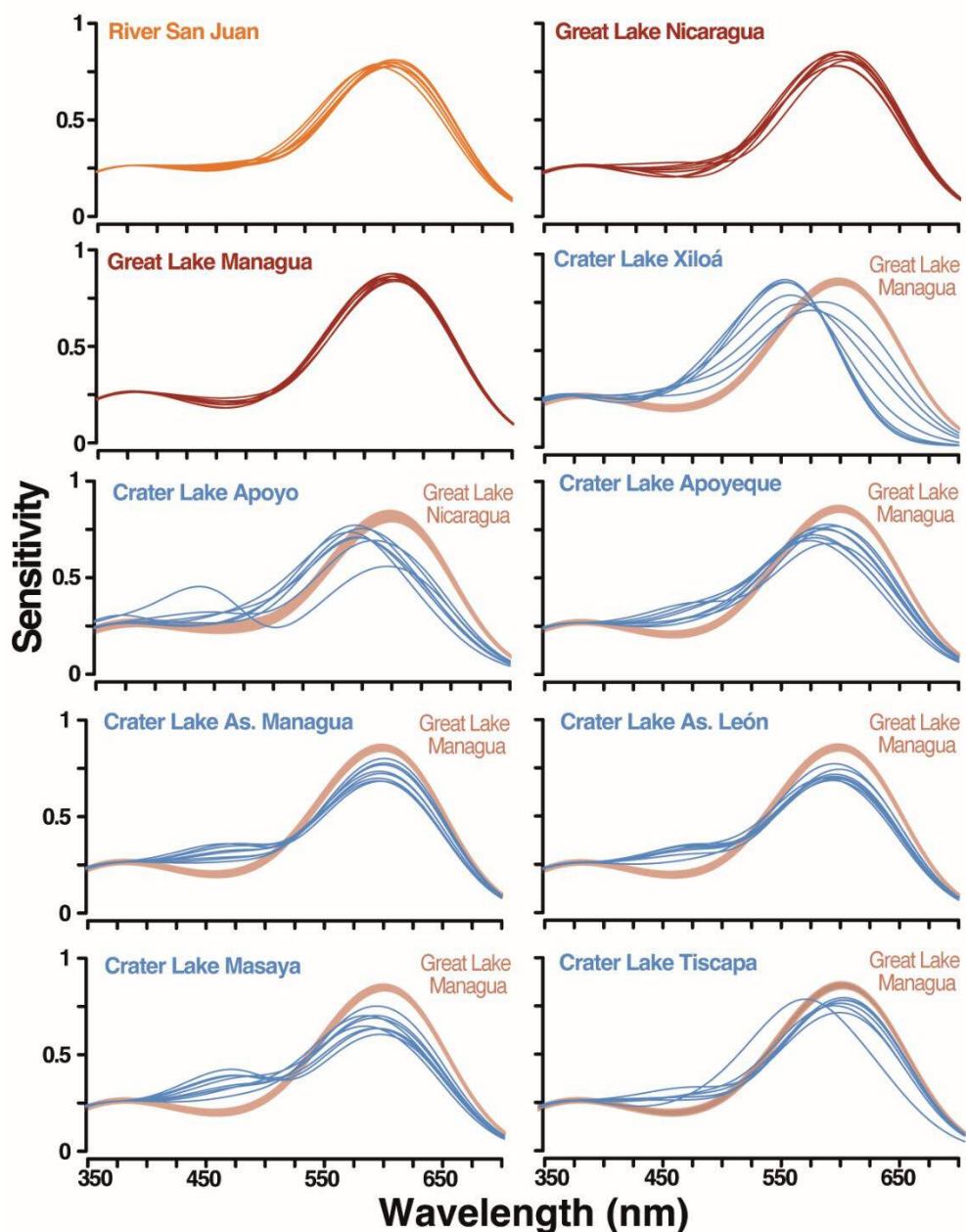


**Figure S5.** Normalized spectral sensitivity assuming A<sub>2</sub>-chromophore usage based on opsin expression (see Fig. 2) of wild-caught individuals based on templates from Govardovskii et al. (2000) and opsin absorbance peaks from Torres-Dowdall et al. (2017). Individual sensitivities are shown as solid lines for each location while shaded area depicts the mean ( $\pm$  SEM) sensitivity of the respective ancestral great lake. Great Lake Managua is considered the predominant source population for the admixed Crater Lake Masaya based on Kautt et. al 2020.

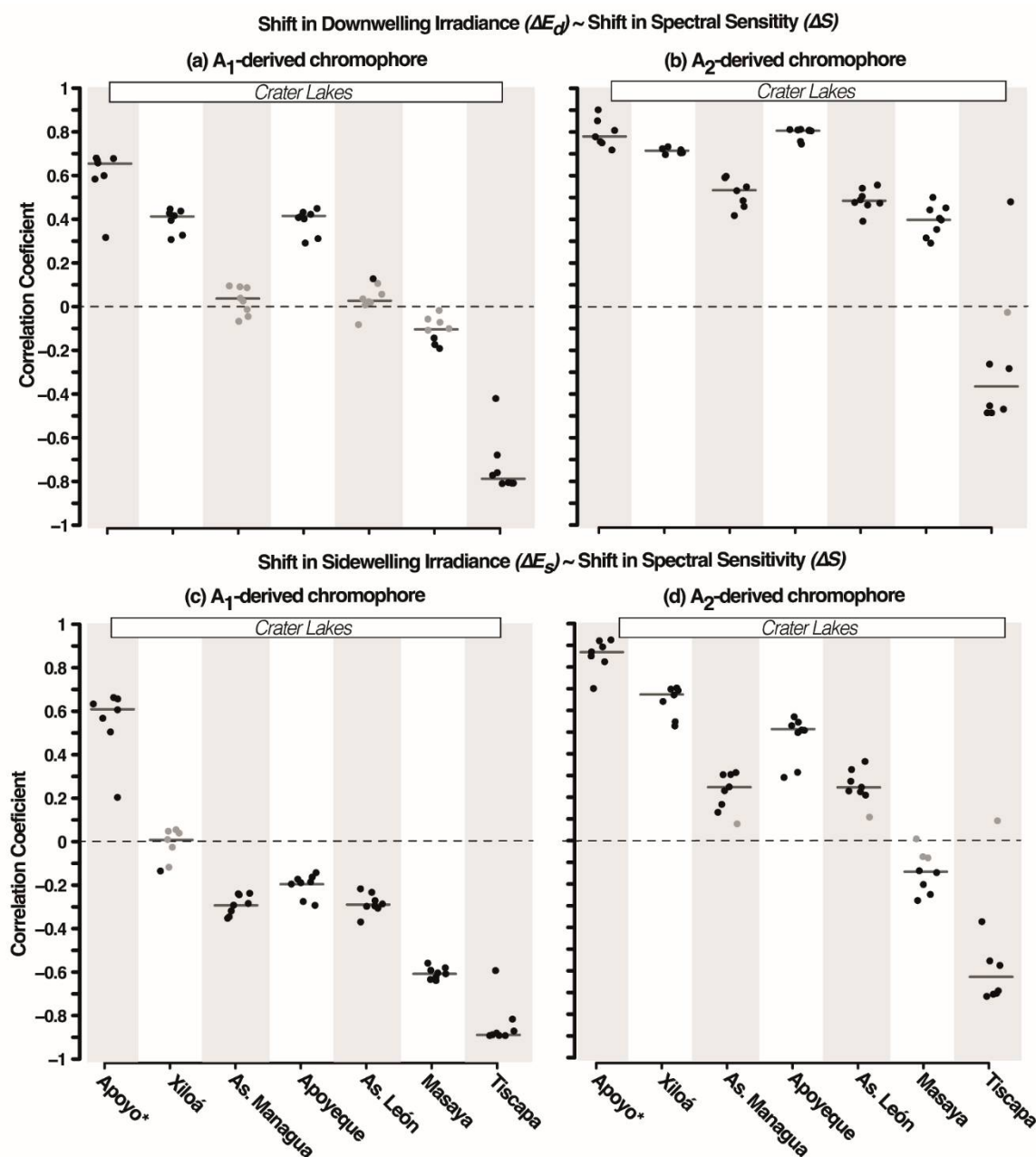


**Figure S6.** Correlation of shift in spectral sensitivity curves ( $\Delta SSC$ ) and normalized spectral irradiance ( $\Delta E$ ) between derived populations and their ancestral population, either great lake Nicaragua (crater lake Apoyo, depict with an asterisk) or great lake Managua. Changes in downwelling irradiance ( $\Delta E_d$ , Fig. 1) for A<sub>1</sub>-chromophore (a) and A<sub>2</sub>-chromophore (b). Changes in sidewelling irradiance ( $\Delta E_s$ , Fig. S2) for A<sub>1</sub>-chromophore (c) and A<sub>2</sub>-chromophore (d). Bars show the median for the correlation coefficients for each population. Black dots ( $p > 0.05$ ) after adjusting for multiple testing using Benjamini-Hochberg FDR. Great Lake Managua is considered the predominant source population for the admixed Crater Lake Masaya based on Kautt et. al 2020.

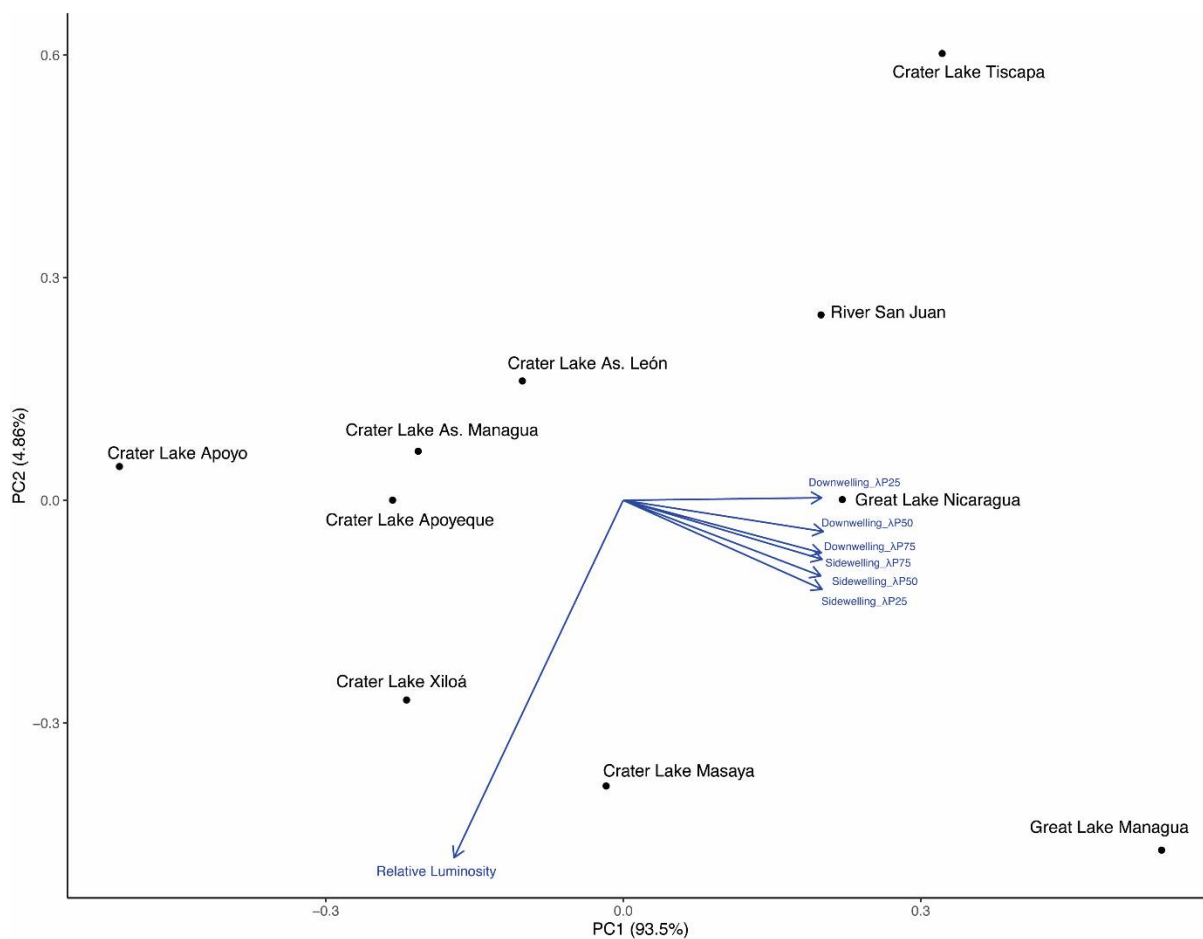


**Figure S7.** Biplot depicting the PCA scores generated from variables of photic conditions of all habitats at one meter depth (Table S4). Arrows represent the loadings of each variable.

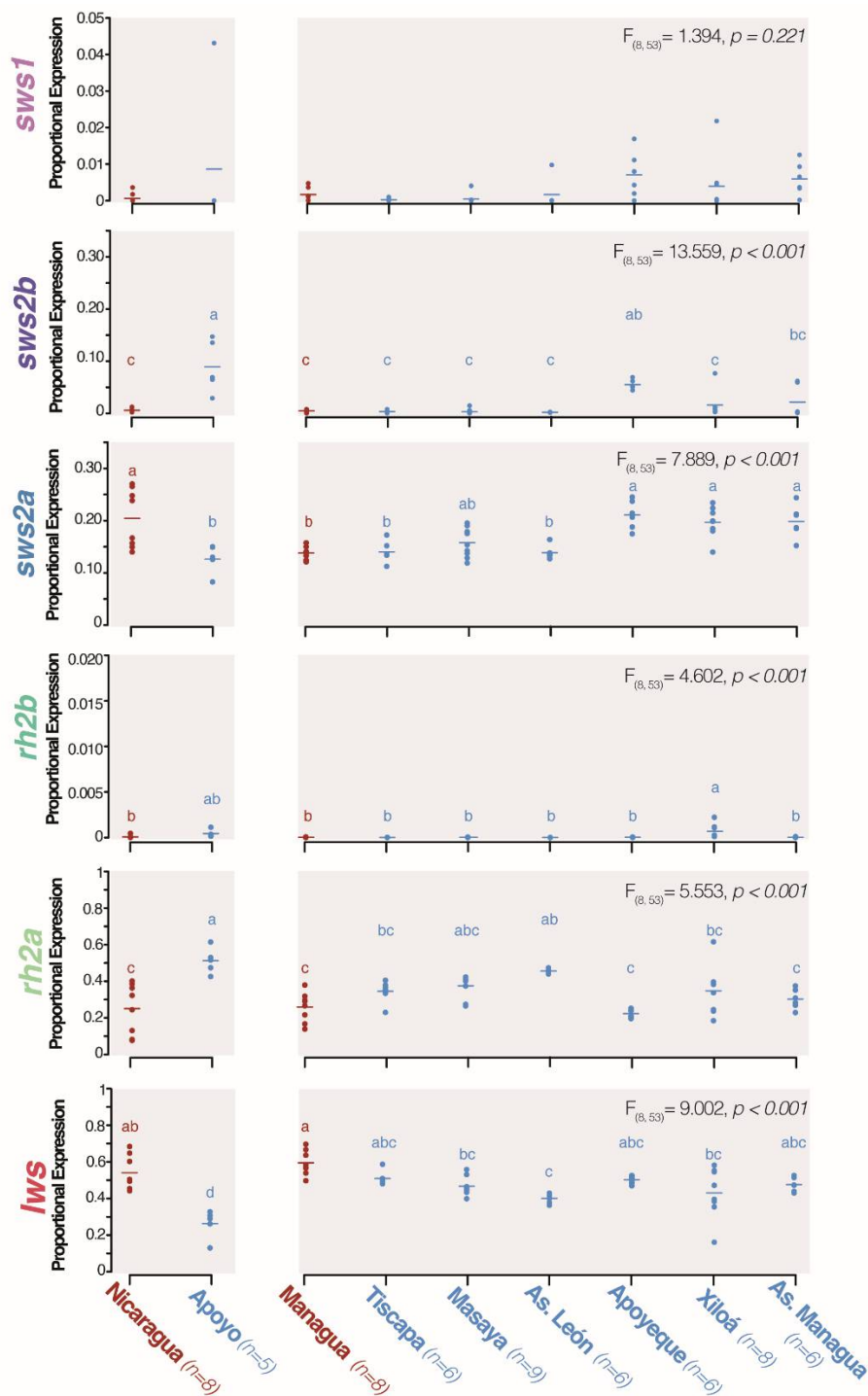


**Figure S8.** Proportional opsin gene expression from lab-reared fish showing groups of derived crater lake (blue) and its respective source great lake (red) within each panel. River San Juan shown in orange. Bars represent the mean value for each population. Upper right corner shows F-values and significance from ANOVA (type II) using location as the predictor variable. Letters display groups based on Tukey's HSD. Great Lake Managua is considered the predominant source population for the admixed Crater Lake Masaya based on Kautt et. al 2018; 2020.

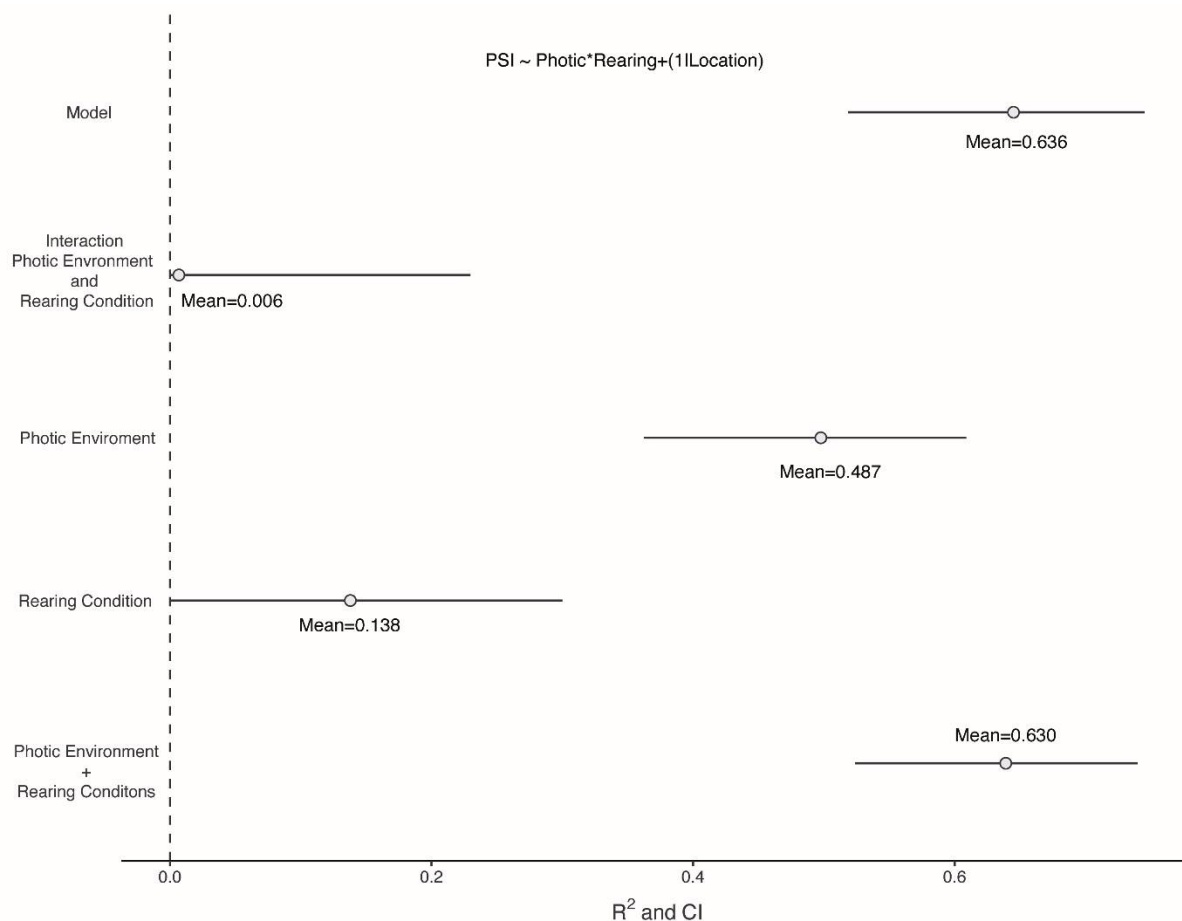


**Figure S9.** Proportion of variance in spectral sensitivity explained by photic environment, rearing condition and its interaction (fixed effects). Dots represent mean R<sup>2</sup> with 95% confidence intervals estimated via bootstrapping (iterations=1000) as described in Stoffel et al. (2021).

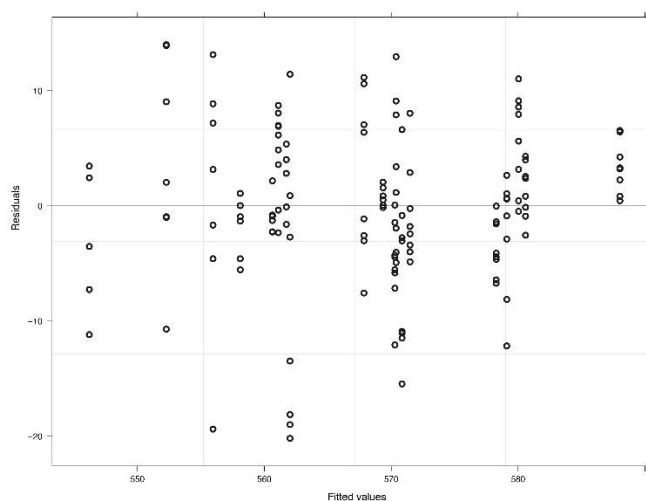


**Figure S10.** Diagnostic plot for linear mixed-effect model shown in Fig. 4a

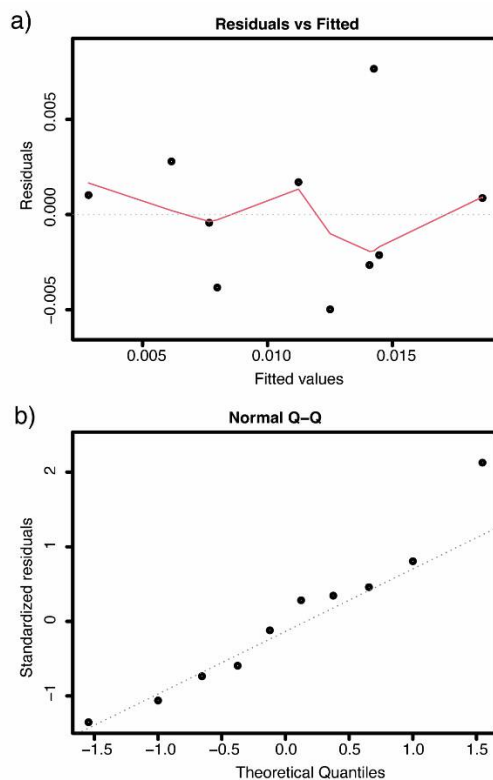


**Figure S11.** Diagnostic plot for linear model shown in Fig. 4b

## References

- Cinelli, C., and C. Hazlett. 2020. Making Sense of Sensitivity: Extending Omitted Variable Bias. *Journal of the Royal Statistical Society Series B: Statistical Methodology* 82:39-67.
- Gingerich, P. D. 1993. Quantification and comparison of evolutionary rates. *American Journal of Science* 293:453.
- Govardovskii, V. I., N. Fyhrquist, T. O. M. Reuter, D. G. Kuzmin, and K. Donner. 2000. In search of the visual pigment template. *Visual Neuroscience* 17:509-528.
- Kautt, A. F., C. F. Kratochwil, A. Nater, G. Machado-Schiaffino, M. Olave, F. Henning, J. Torres-Dowdall et al. 2020. Contrasting signatures of genomic divergence during sympatric speciation. *Nature* 588:106-111.
- Kautt, A. F., G. Machado-Schiaffino, and A. Meyer. 2016. Multispecies Outcomes of Sympatric Speciation after Admixture with the Source Population in Two Radiations of Nicaraguan Crater Lake Cichlids. *Plos Genetics* 12:e1006157.
- . 2018. Lessons from a natural experiment: Allopatric morphological divergence and sympatric diversification in the Midas cichlid species complex are largely influenced by ecology in a deterministic way. *Evolution Letters* 2:323-340.
- Rennison, D. J., G. L. Owens, N. Heckman, D. Schluter, and T. Veen. 2016. Rapid adaptive evolution of colour vision in the threespine stickleback radiation. *Proc Biol Sci* 283.
- Sabbah, S., S. M. Gray, E. S. Boss, J. M. Fraser, R. Zatha, and C. W. Hawryshyn. 2011. The underwater photic environment of Cape Maclear, Lake Malawi: comparison between rock- and sand-bottom habitats and implications for cichlid fish vision. *Journal of Experimental Biology* 214:487-500.
- Stoffel, M. A., S. Nakagawa, and H. Schielzeth. 2021. partR2: partitioning R2 in generalized linear mixed models. *PeerJ* 9:e11414.



Torres-Dowdall, J., M. E. R. Pierotti, A. Harer, N. Karagic, J. M. Woltering, F. Henning, K. R. Elmer et al. 2017. Rapid and Parallel Adaptive Evolution of the Visual System of Neotropical Midas Cichlid Fishes. *Molecular Biology and Evolution* 34:2469-2485.